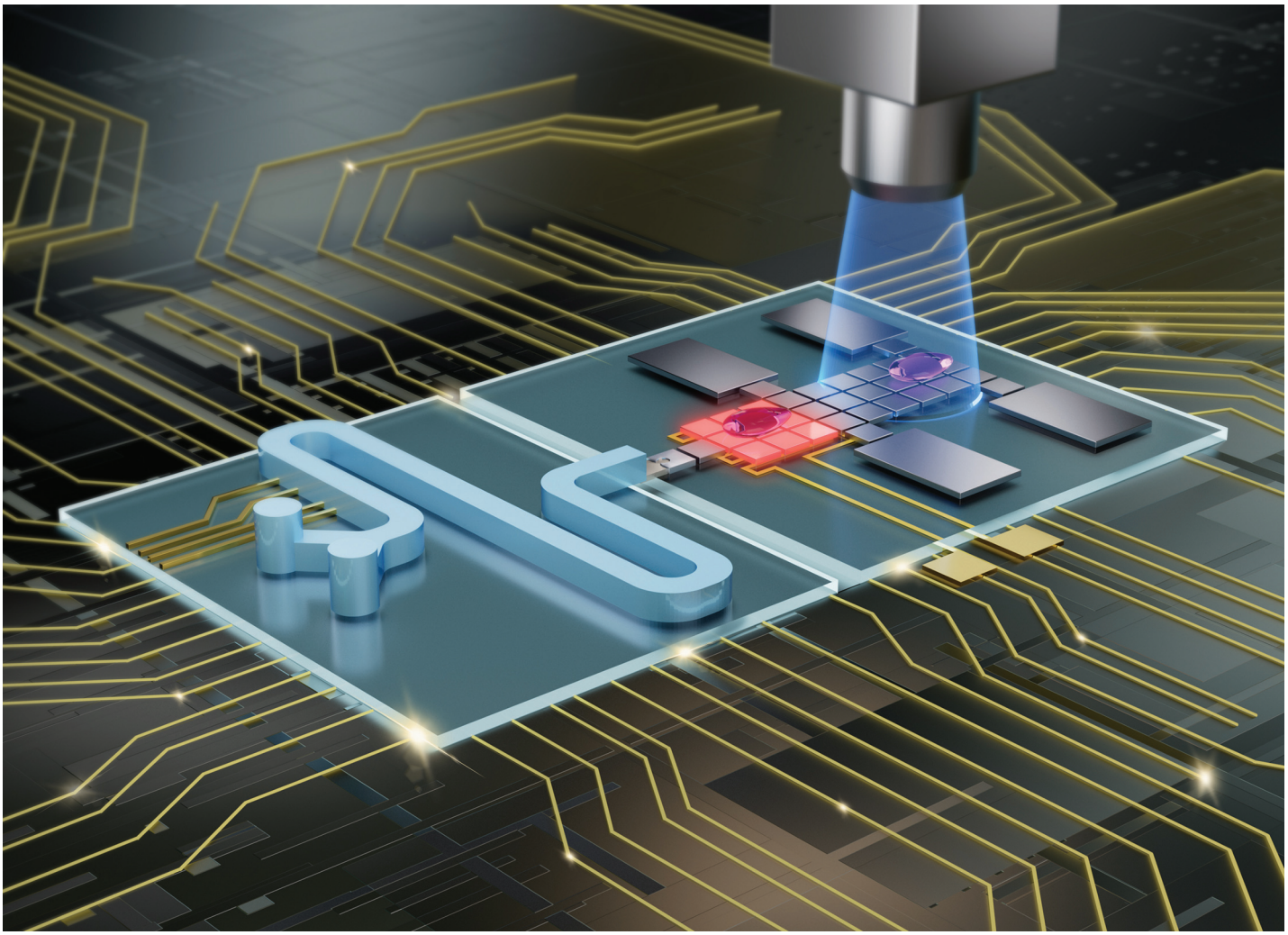

Showcasing research from Professor Mao's laboratory, State Key Laboratory of Transducer Technology, Shanghai Institute of Microsystem and Information Technology, Chinese Academy of Sciences, Shanghai, China.

Combining sensors and actuators with electrowetting-on-dielectric (EWOD): advanced digital microfluidic systems for biomedical applications

Typical forms of a combination of Electrowetting-on-dielectric (EWOD) technology with sensing and other microfluidic manipulation techniques are reviewed from a technical perspective, including the purposes, significance, and biomedical applications of different types of combined microfluidic systems. The image conceptualizes the integration of optical and temperature-control sub-systems on an EWOD chip, as well as the interfacing between EWOD and channel-based microfluidics.

Image reproduced by permission of Shanghai Institute of Microsystem and Information Technology, Chinese Academy of Sciences.

As featured in:

See Hongju Mao *et al.*, *Analyst*, 2023, **148**, 1399.

ROYAL SOCIETY OF CHEMISTRY

rsc.li/analyst

Registered charity number: 207890

Analyst

ROYAL SOCIETY OF CHEMISTRY

CRITICAL REVIEW

View Article Online
View Journal | View Issue

Cite this: *Analyst*, 2023, **148**, 1399

Combining sensors and actuators with electrowetting-on-dielectric (EWOD): advanced digital microfluidic systems for biomedical applications

Zhaoduo Tong, [a,b] Chuanjie Shen, [a,b] Qiushi Li, [a] Hao Yin [a,b] and Hongju Mao *[a]

The concept of digital microfluidics (DMF) enables highly flexible and precise droplet manipulation at a picoliter scale, making DMF a promising approach to realize integrated, miniaturized "lab-on-a-chip" (LOC) systems for research and clinical purposes. Owing to its simplicity and effectiveness, electrowetting-on-dielectric (EWOD) is one of the most commonly studied and applied effects to implement DMF. However, complex biomedical assays usually require more sophisticated sample handling and detection capabilities than basic EWOD manipulation. Alternatively, combined systems integrating EWOD actuators and other fluidic handling techniques are essential for bringing DMF into practical use. In this paper, we briefly review the main approaches for the integration/combination of EWOD with other microfluidic manipulation methods or additional external fields for specified biomedical applications. The form of integration ranges from independently operating sub-systems to fully coupled hybrid actuators. The corresponding biomedical applications of these works are also summarized to illustrate the significance of these innovative combination attempts.

Received 18th October 2022,
Accepted 26th January 2023

DOI: 10.1039/d2an01707e

rsc.li/analyst

1. Introduction

Digital microfluidics is a technology where discrete picoliter- to microliter-scale droplets are actively dispensed and manipulated on a hydrophobic surface.[1] Apart from passive droplet microfluidics such as flow-focusing junctions, hydrodynamic traps, and the SlipChips,[2] DMF enables precise control of an individual droplet, thus providing unparalleled flexibility over

[a]*State Key Laboratory of Transducer Technology, Shanghai Institute of Microsystem and Information Technology, Chinese Academy of Sciences, Shanghai 200050, China. E-mail: hjmao@mail.sim.ac.cn; Fax: +86 21 62511070 8714; Tel: +86 21 62511070 8701*

[b]*Center of Materials Science and Optoelectronics Engineering, University of Chinese Academy of Sciences, Beijing, 100049, China*

Zhaoduo Tong

Zhaoduo Tong is a Ph.D. candidate in Prof. Hongju Mao's group at the Shanghai Institute of Microsystem and Information Technology (SIMIT, CAS). He received his bachelor's degree in Microelectronic Science and Engineering from Central South University. He is mainly engaged in research on digital microfluidics for point-of-care nucleic acid testing.

Chuanjie Shen

Chuanjie Shen is a Ph.D. candidate in Prof. Hongju Mao's group at the Shanghai Institute of Microsystem and Information Technology (SIMIT, CAS). He received his bachelor's degree in Microelectronic Science and Engineering from Jilin University. He is mainly engaged in research on microfluidic biochips for cell sorting and digital microfluidics for single cell analysis.

other microfluidic technologies. In the past decades, multiple actuation principles have been developed to realize DMF, including EWOD,[1,3,4] dielectrophoresis (DEP),[5] magnetic force,[6] photo-actuation principles,[7] acoustic waves,[8] and electro-dewetting,[9] among which EWOD is a well understood and the most commonly applied method in recent studies. Known as a reversible wettability shift induced by an electric charge on a dielectric surface, the EWOD effect is quantitatively described by Lippmann–Young's equation,[10] where the droplet contact angle on the dielectric surface is controlled by an applied voltage. To generate a functional EWOD-based DMF substrate, an electrode array can be patterned by the standard microelectromechanical system (MEMS) process,[11,12] the thin film transistor (TFT) process,[13–15] and inkjet printing,[16,17] or be fabricated on a printed circuit board (PCB),[18,19] along with dielectric layers such as SiO_2 or Al_2O_3 and hydrophobic coatings such as Teflon AF, Cytop and FluoroPel. Droplets are either positioned directly on the open substrate or sandwiched between the bottom substrate and a conductive and hydrophobic top plate as the ground of the DMF device (Fig. 1A). Droplets can then be actively dispensed and manipulated (*i.e.*, transported, merged, and split) on these devices with a typical driving voltage of tens to hundreds of volts (AC or DC) depending on the dielectric properties of the device.

Owing to its simplicity and effectiveness, EWOD has a wide range of applications such as circuit hotspot cooling,[20,21] liquid microlens,[22–24] and electronic ink displays.[5] More importantly, as a fluidic manipulation technique, EWOD is suitable for LOC applications, in which regular biomedical analyses are miniaturized and integrated for point-of-care (POC) diagnosis before treatment.[25] To date, reports on EWOD for LOC applications have covered a variety of biomedical assays, ranging from simple sample preparation to an integrated "sample in, result out" process, from instant manipulation and rapid detection[26] to long-term cell culture and continuous monitoring.[27,28] In addition to the extensive research on LOC applications, EWOD-based DMF is also reaching its mature state in commercialization,[29] as recent disposable EWOD cartridges are being developed for immunoassays,[30,31] single cell sorting,[32] and nucleic acid testing (NAT).[33–36]

However, new challenges emerge for EWOD systems as more sophisticated sample handling actions (*e.g.*, DNA/RNA extraction and single cell isolation), real-time result readout abilities, and higher integration levels are required for practical use under general laboratory or clinical conditions, which cannot be achieved by mere EWOD-driven droplet movements.[10] Therefore, the integration of multiple external fields plays a crucial role in achieving more complex LOC applications and expanding the functionalities of the basic EWOD platform itself. Herein, we briefly review the main approaches for the integration/combination of EWOD with other microfluidic manipulation methods from a technical perspective, as well as the significance of the integration for biomedical (specifically, LOC) applications. For specified purposes, EWOD platforms are generally combined with magnetic, optical, acoustic, thermal, mechanical, and other electrical effects, as well as integrated with sensor units for enhanced sample handling and real-time feedback. Structurally, the combined systems are classified into three categories (Fig. 1B–D) analogous to those of integrated circuits, depending on how coupled the integrated sub-systems are with EWOD actuators, *i.e.*, system-level integration, chip-scale integration, and hybrid actuation.

2. System-level integration

External force fields and the corresponding actuators/sensors may be integrated into EWOD fluidic handling platforms at a system level by positioning exterior sub-systems around the EWOD chip, providing additional control or monitoring for fluidic operation. Such integration requires minimal modification of the existing EWOD device (*e.g.*, thickness, transparency, and heat conductance) but introduces complexity to the external hardware system. Magnetic, optical, and thermal components are typically introduced into EWOD systems in this manner.

Qiushi Li

Qiushi Li is an assistant engineer in Prof. Hongju Mao's group at the Shanghai Institute of Microsystem and Information Technology (SIMIT, CAS). She received her bachelor's degree in Chinese Medicine from Beijing University of Chinese Medicine (BUCM), and master's degree in Laboratory Medicine from RMIT University. Her expertise is in pathology, and she is currently focused on the establishment of disease organoid models.

Hao Yin

Hao Yin is a Ph.D. candidate in Prof. Hongju Mao's group at the Shanghai Institute of Microsystem and Information Technology (SIMIT, CAS). He received his bachelor's degree in Applied Physics from the University of Science and Technology of China (USTC). He is mainly engaged in research on microfluidic biochip engineering and development of application-oriented point-of-care nucleic acid testing devices.

2.1 Magnetic manipulation

The magnetic field is commonly used in liquid handling and is a typical external field to combine with EWOD platforms for practical biomedical analyses. Moreover, magnetic actuation, which performs as a parallel strategy with EWOD in digitized liquid manipulation, relies on magnetic particles (MPs, or magnetic microspheres, magnetic beads) in the target droplets,[37] or magneto-responsive surfaces/liquids,[38] known as "magnetic digital microfluidics[6]". Magnetic particles, on the other hand, are an ideal carrier for affinity-based bioassays in automated systems from the macroscale to the microscale, owing to the high surface-to-volume ratio of the particles and their ease of aggregation and resuspension in liquids. Instead of the droplets being driven around, MPs in EWOD-driven systems usually focus on binding and eventually enriching the biomolecules with high specificity and flexibility.

Early reports on handling magnetic particles on EWOD-based DMF consist of double-plated EWOD chips and regional magnets positioned over or beneath the sandwiched EWOD plates.[39–42] MPs suspended in the liquid droplet are aggregated as the droplet moves partially into the magnetic field, where droplet splitting could be performed by EWOD to trap MPs in a smaller droplet with a high concentration. Furthermore, fully automated "wash" steps of MPs on EWOD are feasible by repeatedly aggregating and resuspending the MPs with wash buffer.[43] Under a similar principle, the combination of EWOD and MP handling has enabled integrated and miniaturized biomedical assays such as cell manipulation,[44,45] immunoassays,[31,46–52] mass spectrometry,[53] nucleic acid extraction[54–57] and sequencing.[34,58,59] Meanwhile, efforts are also made to enhance the sample handling and detection abilities of EWOD platforms using MPs.

Shah *et al.*[60,61] proposed an MP purification method *via* a surfactant-mediated fluidic conduit between the source and target droplets, which minimizes diffusion and mixing of the two droplets. Chen *et al.*[62] enabled intra-droplet MP manipulation by adding current-carrying electric wires on EWOD plates as micro-electromagnets. Huang *et al.*[63] demonstrated an efficient collection of MPs at a low concentration through an asymmetric electrode design. Guo *et al.*[64] developed a bi-directional separation method for MPs to achieve their high retention efficiency and washing efficiency (Fig. 2A). Jin *et al.*[50] realized the "one-to-three" droplet splitting method on an EWOD platform (*i.e.*, splitting one droplet into three sub-droplets simultaneously) by placing a smaller active electrode in the middle of two major electrodes dragging the droplet to opposite directions. Such a design reduces the magnetic force to retain MPs in the middle droplet and enables more stabilized MP handling (Fig. 2B).

2.2 Optical manipulation

Combining optical components with the EWOD technique is an effective approach to enhance fluidic handling functionalities in DMF. The complexity of the optical actuators in DMF mainly lies in exterior systems instead of the chip structure. In the past decades, principles such as optoelectrowetting, optical tweezers, and optoelectronic tweezers have been implemented for droplet actuation and particle manipulation on EWOD platforms.[7,65]

Optoelectrowetting (OEW) is a modification of traditional electrowetting for droplet actuation *via* a combined external voltage supply and light (laser) source. Chiou *et al.*[66] established the first OEW device by adding a photoconductor (hydrogenated amorphous silicon or a-Si:H) layer under the SiO_2 dielectric of a typical EWOD substrate (Fig. 2C). While electrodes are active, voltage bias on the dielectric layer and hence the droplet contact angle are controlled by the photoconductor layer, whose local impedance is governed by an applied laser beam. OEW overcomes the limitation of circuiting in EWOD and allows for continuous droplet manipulation on a dielectric surface *via* a patterned light source[67–69] (Fig. 2D). Both enclosed (double-plate)[66,70–73] (Fig. 2C) and open (single-plate)[74–76] (Fig. 2D) versions of this OEW technique are demonstrated. However, reports on OEW actuation in LOC applications are rare compared to conventional EWOD actuation.

On the other hand, optical tweezer (OT) and optoelectronic tweezer (OET) techniques aim at the manipulation of dielectric microparticles in a suspension. The earliest reports on OTs can be traced back to Ashkin *et al.*,[77,78] in which particles can be trapped three-dimensionally by a laser beam directly focused on the particle.[79] For OT applications, Decrop *et al.*[80] realized OT integration on an EWOD device for the manipulation of single MPs seeded in a microwell array by selectively trapping and relocating individual MPs from one microwell to another. Kumar *et al.*[81] expanded this system for bacterial cell sorting, where MPs, which are further seeded with antibodies, are used for capturing bacteria (Fig. 2E). However, OETs generally have a different working principle, which was first demonstrated by Chiou *et al.*[82] The principle of OETs can be briefly described as the light-induced DEP effect, where a laser beam focuses on photoconductive materials in the device substrate and triggers the local DEP effect. OETs largely reduce the laser intensity required for particle manipulation compared to OTs and have a similar double-plate structure to EWOD, making

Hongju Mao

Hongju Mao is a Professor at the Shanghai Institute of Microsystem and Information Technology (SIMIT, CAS). She received her PhD degree from the University of Chinese Academy of Sciences and has been a visiting scholar at the University of Leeds. Her research interests include microsystems for liquid biopsy, point-of-care diagnosis, biochemical sensors, and in vitro *disease models.*

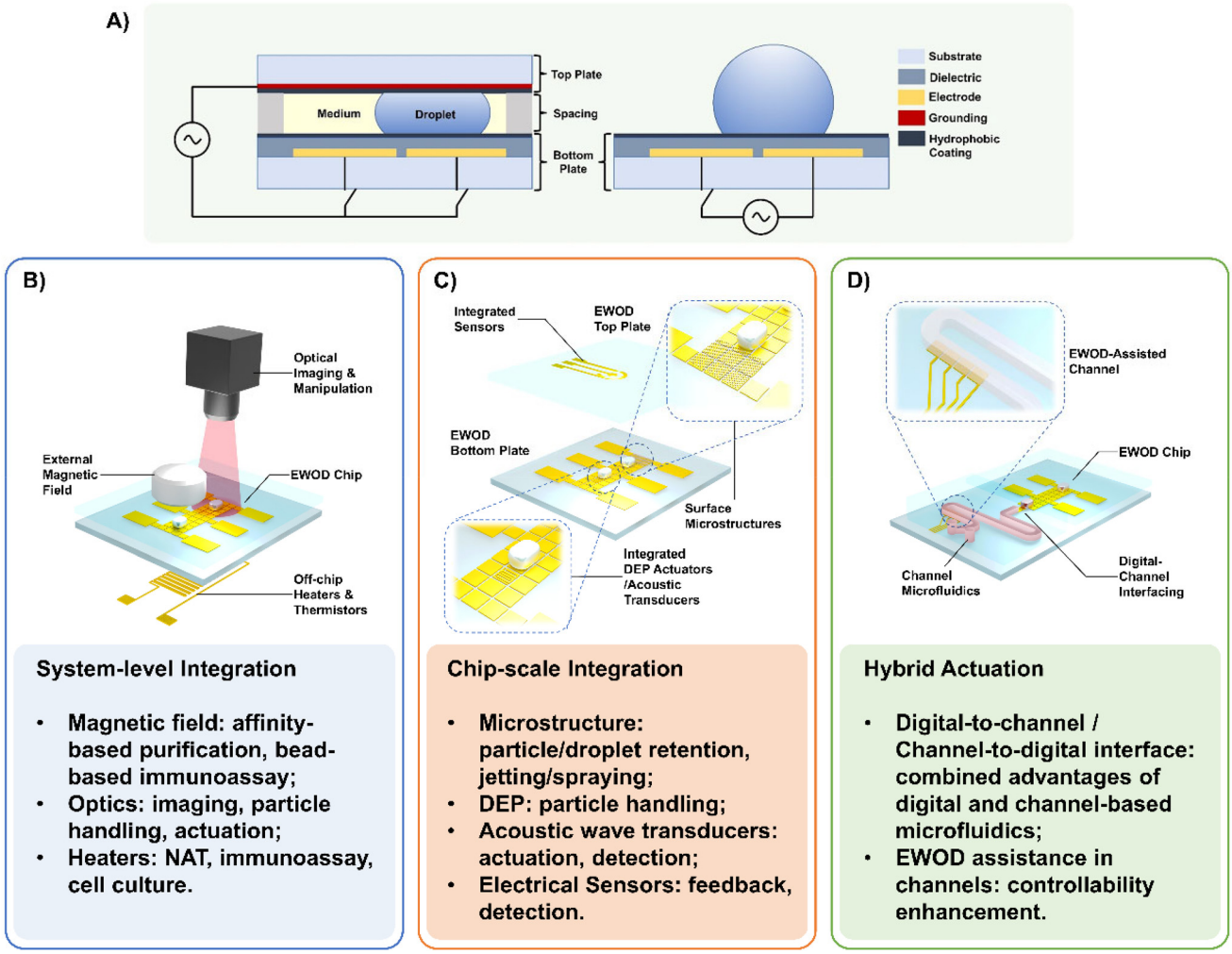

Fig. 1 Classification of the combination forms of EWOD-based DMF systems and their functionalities. (A) Cross-sectional schematic of typical enclosed double-plated (left) and open single-plated (right) EWOD chip structures; (B), (C) and (D) conceptual models of combined EWOD systems classified as system-level integration, chip-scale integration and hybrid actuation, respectively, depending on their degree of coupling. System-level integration: exterior systems are built in addition to typical EWOD for improved non-contact control. Chip-scale integration: built-in components and/or modifications are added to EWOD chips during fabrication. Hybrid actuation: interaction of EWOD with conventional channel-based microfluidics is exploited, where systems include both EWOD and pumping actuators. NAT: nucleic acid testing; DEP: dielectrophoresis; EWOD: electrowetting-on-dielectric.

OETs an effective tool to combine with EWOD actuation. For OET applications, Shah *et al.*[83] established an integrated EWOD-lateral-field OET (LOET) device and realized cell collection within an EWOD-actuated droplet. LOETs were developed as a single-plate version of OETs rather than a double-plate as in EWOD, allowing for a minor modification to the EWOD structure on another substrate (Fig. 2F). Valley *et al.*[84] integrated OEW actuation with OET particle manipulation. This unified OEW–OET device (Fig. 2G) enables continuous particle concentration and liquid handling compared to EWOD–DEP devices (see section 3.2) with predefined patterns of actuators. Huang *et al.*[85] combined OETs with real-time imaging *via* a CCD/CMOS sensor array and implemented cell sorting. Recently, Zhang *et al.*[86] demonstrated OET-driven microscale gears, racks, and other micro-mechanisms by light patterns, extending the flexibility of OETs as a non-contact manipulation method in digital microfluidics (Fig. 2H).

In addition to general purposes such as droplet and particle handling, external optical equipment may be used for more specific situations. Lamanna *et al.*[12] performed single-cell omics on an EWOD platform, where individual cells are identified and lysed by an external laser pulse prior to further studies of cellular contents such as proteins and DNA (Fig. 2I).

2.3 Temperature control

It is crucial to maintain one temperature, or cycle different temperatures for certain biochemical reactions. Hence, temperature control abilities are essential for DMF systems in integrated biomedical applications. So far, numerous temperature-sensitive purposes performed on EWOD platforms are present,

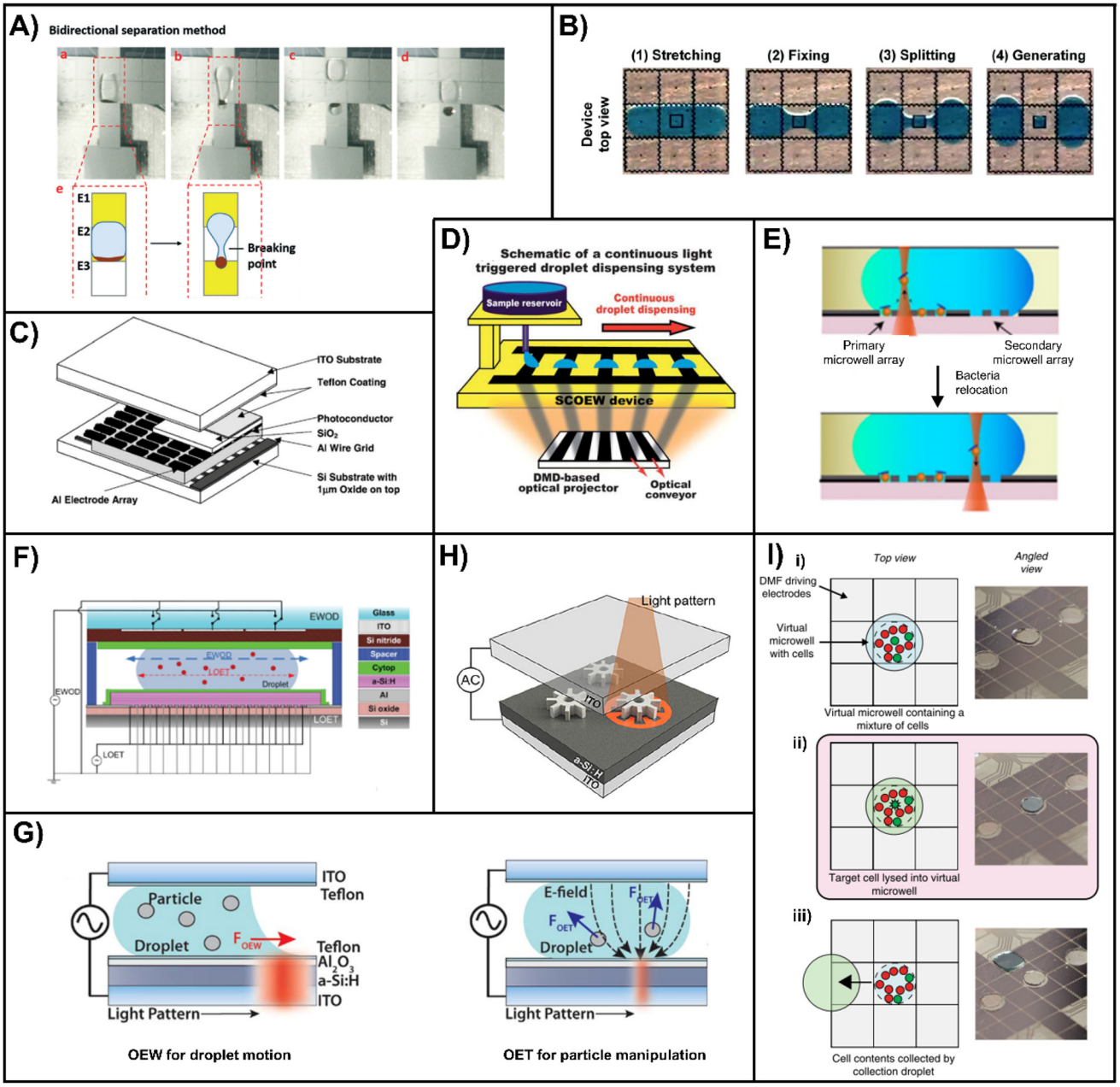

Fig. 2 Magnetic and optical manipulation of samples for DMF. (A) Bidirectional separation of magnetic particles on the EWOD platform using external magnet and sequential electrode activation. Reproduced with permission from ref. 64. Copyright 2020, the Royal Society of Chemistry. (B) "One-to-three" droplet separation where magnetic particles are retained at the center. Reproduced with permission from ref. 50. Copyright 2021, the Royal Society of Chemistry. (C) Schematic structure of a double-sided OEW device with an electrode array. ITO: indium-tin oxide. Reproduced with permission from ref. 66. Copyright 2003 Elsevier. (D) Schematic of the single-sided continuous optoelectrowetting (SCOEW) device. Droplets are manipulated at an arbitrary position on the device surface by an optical projector. Reproduced with permission from ref. 67. Copyright 2010, the Royal Society of Chemistry. (E) Cross-sectional view of bacterial relocation *via* an optical tweezer in an EWOD droplet. Reproduced with permission from ref. 81. (F) Cross-sectional schematic of a lateral-field OET (LOET) integrated on EWOD for particle manipulation. Cytop: a hydrophobic coating; a-Si:H: hydrogenated amorphous silicon. Reproduced with permission from ref. 83. Copyright 2009, the Royal Society of Chemistry. (G) Schematic diagram of a unified platform for OEW and an OET, where the OEW force drives the droplet and the OET force manipulates particles within the droplet. Reproduced with permission from ref. 84. Copyright 2011, the Royal Society of Chemistry. (H) Schematic of an OET device with light-driven micro-gears. Reproduced with permission from ref. 86. (I) An EWOD platform with 2D cell culture and laser-induced single cell lysis. From (i) to (iii): the process of the assay, including cell culture in the EWOD chip, selective lysis of the target cell by a laser, and collection of the lysed cell contents. Descriptions of the virtual microwell can be found in Fig. 4A and in section 3.1. Reproduced with permission from ref. 12.

including cell culture,[87] polymerase chain reaction (PCR),[35,36,44,88–94] isothermal amplification,[14,33,95–99] and immunoassays.[100]

Temperature control units are typically composed of microheaters/coolers, thermal sensors, and microcontrollers to form a close-looped control. Distinct strategies are adopted for integrating temperature control capability on the EWOD platform, namely, (1) placing heaters and sensors externally in the chip holding structures (system integration),[33,88,97–106] (2) fabricating heaters and/or sensors on EWOD substrates (chip-scale integration),[57,89,92–94,96,107–109] and (3) using EWOD electrodes for multifunctional heating/sensing.[14,110–114] For strategy (1), Shen *et al.*[100] patterned a resistive microheater on a separate substrate (on the right) stacked and aligned with the EWOD bottom plate (on the left) (Fig. 3A). Narahari *et al.*[33] developed a portable DMF platform for sampling and isothermal amplification of viral RNA, where replaceable EWOD cartridges (not shown) are clamped between the top and bottom heater plates during the amplification (Fig. 3B). Hu *et al.*[97] also used a separate temperature control unit in an integrated DMF system for nucleic acid detection based on loop-mediated isothermal amplification (LAMP). Sathyanarayanan *et al.*[105] used inkjet-printed heating wires adhered to the EWOD bottom plate in their study. For strategy (2), Chang *et al.*[92] fabricated EWOD bottom plates with an additional metal layer for temperature control. Norian *et al.*[108] demonstrated miniaturized EWOD and quantitative PCR (qPCR, real-time PCR) based on the complementary-metal–oxide semiconductor (CMOS) process, as some individual electrodes possess integrated heaters and sensors. For strategy (3), Kalsi *et al.*[14] performed DNA recombinase polymerase amplification (RPA) on a TFT array EWOD platform, where the indium-tin-oxide (ITO) top plate is connected to a second source for Joule heating while grounded. Nampoothiri *et al.*[112] used EWOD electrodes for direct Joule heating under high-frequency (ω) signals (Fig. 3C). Nelson *et al.*[113,114] designed a specialized serpentine actuation electrode for multifunctioning as a heater while connected to a heating circuit. The multifunctional heater is used to accelerate liquid drying and matrix crystallization for mass spectrometry.

Decoupling temperature control units from the EWOD chips (*i.e.*, strategy 1) is more frequently observed in the recent literature, as these control units possess more complete functionalities and are closer to the actual point of care (POC) applications. By comparison, in strategy 2, integrating heaters and thermal sensors on EWOD substrates results in increased fabrication cost, limited flexibility, and extra complexity to the system, whereas the multifunction strategy (strategy 3) hinders simultaneous actions of droplet manipulation and heating.

Specifically for assays requiring cycling temperatures (*i.e.*, PCR), another two different approaches are developed and validated: (1) continuously adjust the set value of a sole heater on the anchored target droplet,[35,36,44,103,104] as performed in commercial thermal cyclers; and (2) shuttle the target droplet between different temperature regions on the chip by electrowetting.[88,89,101,102,115] For approach (1), Rival *et al.*[44] realized total messenger RNA (mRNA) extraction from a human cell line and reverse transcription quantitative PCR (RT-qPCR) assay, in which parallel PCR blocks are designed on the EWOD chip for 20 individual droplets to settle (Fig. 3D). For approach (2), Ho *et al.*[88] reported a PCB-based EWOD cartridge for RT-qPCR detection of viral RNA, where 95 °C and 60 °C regions on the PCB are established respectively for the required denaturation and annealing procedure in a thermal cycle (Fig. 3E). Li *et al.*[101] demonstrated EWOD-based DNA melt curve analysis comparable to the traditional qPCR method, by dispensing the columns of picoliter-scale microdroplets from EWOD-driven mother droplets along a temperature gradient generated by a spatially gapped heat source and a heat sink (Fig. 3F). As determined by their distinct characteristics, approach (1) shows simplicity over chip design but requires good heat conductance of EWOD substrates to enable rapid heating or cooling of the sample, whereas approach (2) relieves the heating configuration at the cost of higher requirements of the overall reliability of EWOD actuation for droplet shuttling.

3. Chip-scale integration

Chip-scale integration refers to EWOD systems that have additional components fabricated on the chip structure such as detection sensors and dielectrophoretic actuators, which often causes extra complexity to the chip fabrication process, and the compatibility of the additive material and EWOD structure is inevitably considered under such circumstances. However, the combination of additive structures with the EWOD chips is necessary when precision or direct contact with samples is required for some applications that involve sensors. Also, modifications to the chip structure allow for specialized functionalities and maintain the exterior system in a compact and user-friendly state. Representative criteria for chip-scale integration include chip surface modification, integration of sensors, and combination with dielectrophoretic actuators.

3.1 Surface microstructure/modification

One of the significant advantages of traditional channel-based microfluidic chips for LOC applications is the use of patterned microstructures or modifications as processing units in the flow channel. Such structures are critical for mixing,[116] sample isolation & enrichment,[117] capture,[118] detection,[119] and other purposes at the microscale. As an active actuation approach, digital microfluidics, however, no longer need microstructures for basic fluidic manipulation. Nevertheless, structures fabricated by micropatterning may still play a crucial role in the EWOD systems for specialized key sample manipulation steps, which combine the specialties of these microstructures with the flexibility of the EWOD platform.

For surface modification, the patterning of hydrophobic/hydrophilic sites on the EWOD chip surface is a strategy widely accepted for droplet dispensing and the anchoring of cells and analytes of interest. Barbulovic-Nad *et al.*[120] first demonstrated adherent (2D) cell culture on the EWOD chip

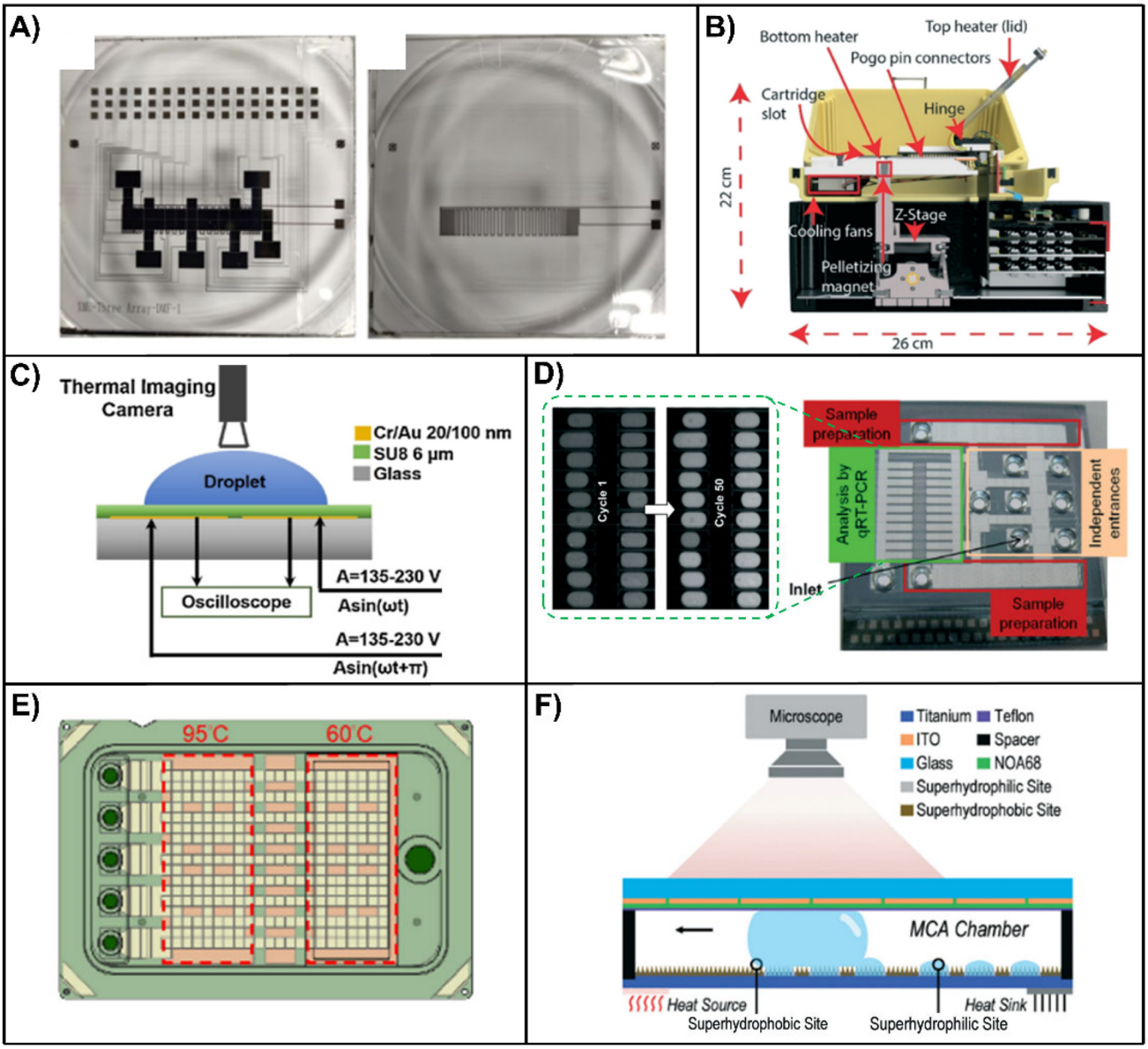

Fig. 3 Integration of temperature control on EWOD. (A) Photograph of a serpentine heating wire (on the right) stacked with an EWOD bottom plate (on the left) for temperature control. Reproduced with permission from ref. 100. Copyright 2021 American Chemical Society. (B) Cross-sectional view of an EWOD hardware system for LAMP, where the chip (not shown) is sandwiched between two separate heaters. The motorized Z-stage and the pelletizing magnet enable control of MPs for nucleic acid extraction. Reproduced with permission from ref. 33. Copyright 2022, the Royal Society of Chemistry. (C) Schematic of an EWOD heater using high-frequency (ω)-induced Joule heating. Reproduced with permission from ref. 112. Copyright 2018 Elsevier. (D) Photograph and fluorescent (FAM) image of an EWOD chip for multiplexed qPCR. qRT-PCR (RT-qPCR): reverse transcription quantitative polymerase chain reaction. Reproduced with permission from ref. 44. Copyright 2014, the Royal Society of Chemistry. (E) Top view of an EWOD cartridge (chip) for qPCR with two temperature (60 and 95 °C) zones generated by external heaters (not shown). Reproduced with permission from ref. 88. (F) Schematic of a DNA melt curve-analyzing device with a heat gradient along the droplet path. ITO: indium-tin oxide; MCA: melt curve analysis; NOA68: a UV adhesive as an insulation layer. Reproduced with permission from ref. 101. Copyright 2022, the Royal Society of Chemistry.

surface. As the Teflon AF surface does not support cell adhesion, islands of extracellular matrix (ECM) proteins are coated on the surface prior to cell culture. Eydelnant *et al.*[11] improved the cell culture ability of an EWOD device by a process known as Teflon liftoff, creating on a Teflon-coated device surface some hydrophilic sites, or "virtual microwells" (Fig. 4A), which is an approach adopted in numerous subsequent works[12,121] (see also Fig. 2I). Likewise, Xu *et al.*[122] realized single-cell RNA sequencing on an EWOD device, where single-cell encapsulated droplets are passively dispensed by moving the cell suspension droplets over a small hydrophilic site and leaving a small droplet containing a single cell, pro-

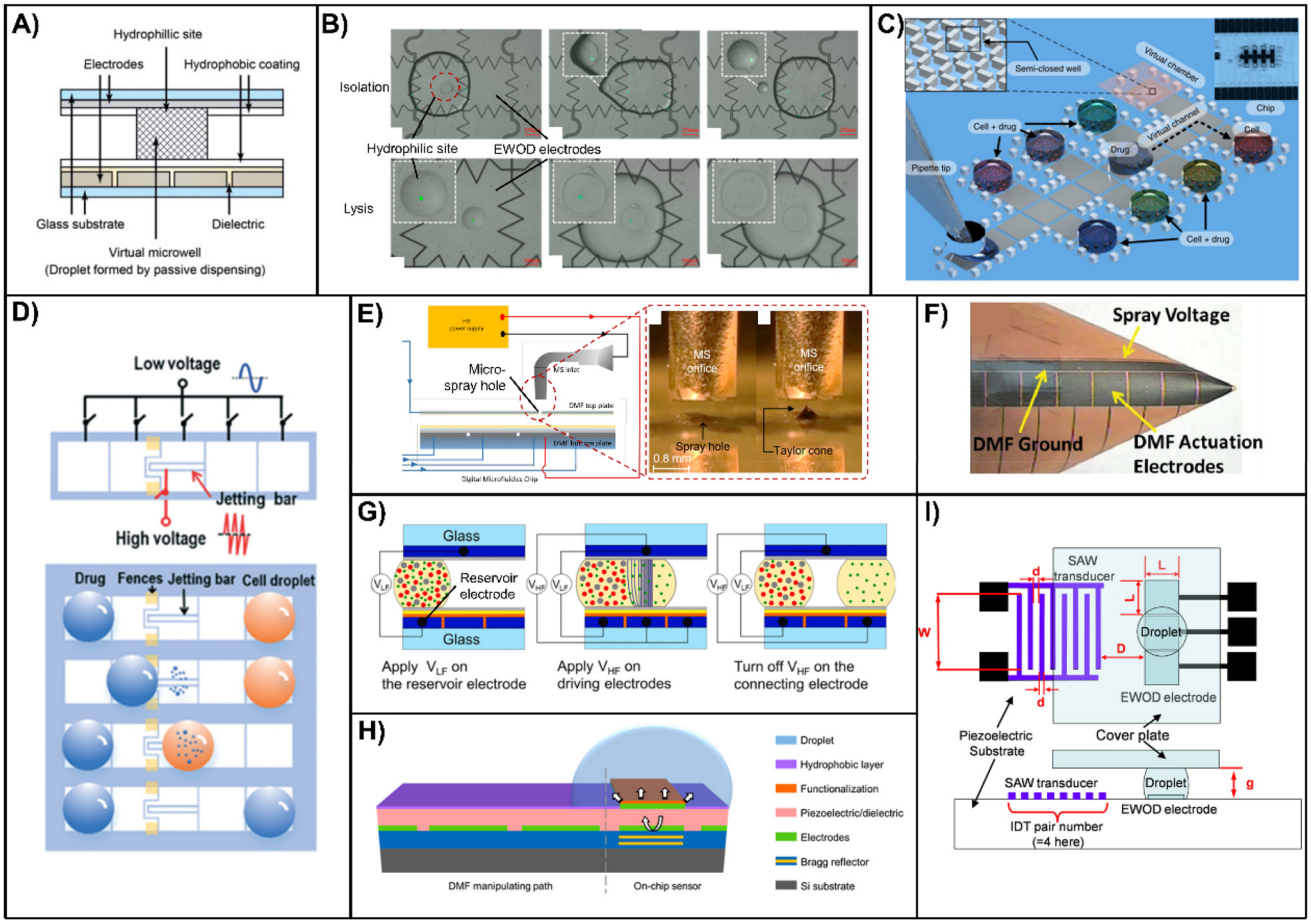

Fig. 4 Combination of microstructures, DEP and acoustic wave actuators with EWOD chips. (A) Schematic diagram of a double plated EWOD chip with a hydrophilic site on the top plate and a virtual microwell for cell culture. Passive dispensing: the process in which an EWOD-driven droplet passes through a hydrophilic site, leaving a column-shaped sub-droplet. Reproduced with permission from ref. 11. Copyright 2012, the Royal Society of Chemistry. (B) Images of a hydrophilic site on an EWOD bottom plate for single cell isolation and lysis. Multiple cells (green dots) are transferred by EWOD in a droplet, and a single cell is isolated at the hydrophilic site. Reproduced with permission from ref. 122. Copyright 2018 American Chemical Society. (C) Conceptual diagram of a single cell trapping semi-closed microwell array on EWOD (pink, upper left). Reproduced with permission from ref. 125. (D) Schematic of a jetting-based drug dispenser in which satellite drops are formed using a high voltage. Reproduced with permission from ref. 128. Copyright 2021, the Royal Society of Chemistry. (E) Schematic diagram (left) and images (right) of an integrated micro-spray hole on the EWOD top plate for in-line electrospray ionization mass spectrometry (ESI-MS). Reproduced with permission from ref. 130. Copyright 2022 American Chemical Society. (F) Image of a flexible microfluidic origami device for ESI-MS. Reproduced with permission from ref. 131. Copyright 2013, the Royal Society of Chemistry. (G) Working principle of an EWOD–DEP chip for plasma separation from whole blood. V_{HF}: high-frequency voltage for DEP; V_{LF}: low-frequency voltage for EWOD. Reproduced with permission from ref. 142. Copyright 2022 Elsevier. (H) Cross-sectional schematic of an EWOD chip integrated with a bulk acoustic wave (BAW) sensor for a label-free immunoassay. The piezoelectric substrate for the sensor also performs as the dielectric layer for EWOD. Reproduced with permission from ref. 147. Copyright 2018 American Chemical Society. (I) Top view (top) and cross-sectional view (bottom) of a double-plate EWOD device interfaced with surface acoustic wave (SAW) transducers. EWOD electrodes and SAW transducers share the same piezoelectric substrate. *W*, *d*, *D*, *L*, *g*: critical parameters for the EWOD and SAW electrodes. Reproduced with permission from ref. 151. Copyright 2012 AIP Publishing.

vided an appropriate initial cell concentration is used (Fig. 4B). Witters *et al.*[123] used the Teflon patterning technique to create a microwell array for trapping of single magnetic particles (MPs) for fluorescence detection. Li *et al.*[101] replaced conventional Teflon coating on the surface of their EWOD chips with novel superhydrophobic coating and patterned superhydrophilic microwells to maximize the wettability contrast between the microwell and the surrounding, thus realizing efficient dispensing of an array of satellite droplets for DNA melt curve analysis (Fig. 3F).

For microstructures, patterning substantial micropillars above the actuating electrodes is a facile approach to provide extra control over the sample. Au *et al.*[124] developed an EWOD three-dimensional (3D) cell culture structure based on collagen gel on an EWOD platform. The media exchange process in 3D cell culture proved challenging as spheroids (along with the collagen matrix) are free-floating within the media droplet. Hence, SU-8 micro-posts are fabricated on the EWOD dielectric layer as a retention barrier to form semi-closed wells. Zhai *et al.*[125,126] established a single cell trapping method on DMF,

which also uses an SU-8 fence array to form rectangular semi-closed wells for arrayed single cell capture and culture (Fig. 4C). Drug toxicity assays can be conducted on such devices with clear readings of cell viability due to drug action, as individual cells are confined to each micropatterned well. Ruan *et al.*[127] presented another active single cell capture approach on an EWOD platform, where a cell suspension droplet is manipulated around a butterfly-shaped micro-post array. The array traps only a single cell at a time, allowing for further washing steps to remove surplus cells in the suspension droplet. Another work presented by Zhai *et al.*[128] demonstrated a micro drug dispenser based on EWOD droplet ejection, in which a pulse wave actuation signal is applied to the reservoir droplet by a jetting bar electrode and causes the generation of multiple satellite drops. Micro-posts are fabricated as fences around the reservoir droplet to prevent the drifting of the reservoir droplet under the actuation signal (Fig. 4D).

Apart from the micropillars, another practical microstructure for the EWOD chips is through holes. Besides acting as general liquid inlets/outlets, through holes on the EWOD substrates are sometimes used for specialized purposes. Bender *et al.*[129] demonstrated the formation of cell spheroids on an EWOD chip. The bottom plate of the chip contains through-holes (1–3 mm in diameter) to form hanging drops, in which the individual cells may aggregate and form cell spheroids spontaneously. Das *et al.*[130] combined the electrospray ionization (ESI) method for mass spectrometry (MS) with DMF using a dry-etched micro-hole (10–40 μm in diameter) on the EWOD chip top plate. The MS orifice is positioned above the top plate in proximity to the micro-hole. Therefore, when a droplet containing samples is parked under the micro-hole, a Taylor cone for electrospray can be generated through the micro-hole by applying a pulsed high voltage between the EWOD bottom electrode and the MS orifice (Fig. 4E).

In particular, for EWOD chips built on flexible substrates, the folding of the substrates provides a unique opportunity to achieve specific functionalities. Kirby and Wheeler[131] developed a "microfluidic origami" device for the ESI. A conical shape is folded out of a single polyimide EWOD substrate, and the cone apex includes both the EWOD actuation electrodes and a thin wire for the electrospray voltage. A Taylor cone is generated through the apex when a high DC voltage is applied to the droplet in the folded cone apex (Fig. 4F).

Overall, the surface modification and microstructure on EWOD chips provide DMF systems with the ability to constrain the manipulated droplet or the samples within. This strategy is efficient under the circumstances such as the partitioning of droplets and retention of large particles such as cells and MPs. Compared with other chip-scale integration strategies, the surface microstructure/modification is a passive method that requires no extra establishments in the external system. The mechanical constraints provided by the modification are relatively reliable and friendly to biological samples. In addition, the fabrication of the microstructure is well compatible with the cleanroom process, where UV-curable gels (*e.g.*, SU-8 photoresist) may perform as both the microstructure and dielectric materials. However, the release of samples from the microstructure or modification cannot be efficiently executed by EWOD driving without additional force fields. This issue makes the EWOD systems with surface microstructures or modifications inconvenient for repeated operation, and limits the potential of the sample for subsequent analyses. Meanwhile, although modifications are applicable for most EWOD substrates, further investigations are required to establish facile fabrication methods of microstructures on low-cost substrates such as polymer substrates or PCB.

3.2 Dielectrophoretic manipulation

Electrophoresis is a phenomenon where charged particles are subjected to an electric field, while DEP describes polarization and directional movement of insulated particles in a non-uniform field,[132] which is a practical approach accepted in microfluidics for liquid handling and manipulation of biological particles.[133,134] As presented in previous studies, both the liquid handling capability of DEP and electrowetting (EW) contribute to liquid movement in electromechanically induced (*i.e.*, external voltage-based) DMF systems.[135] As either effect may take major responsibility for liquid handling, devices with DEP as the dominant effect are referred to as liquid dielectrophoresis (LDEP)-based DMF.[136]

Besides being an independent actuation principle for DMF, DEP may be tuned for the capture and separation of specific particles in the sample fluid, thus performing as a complementary tool in EWOD-driven devices. Such EWOD–DEP platforms possess enhanced sample handling functionality, while no extra complex fabrication process is required to create these platforms for chip-scale integration.

Fan *et al.*[137] performed both the EWOD and DEP manipulation on a double-plate electrode array platform, in which EWOD controls a conductive droplet (water phase), and DEP manipulates a dielectric droplet (oil phase), expanding the controllability of DMF to non-conductive liquids on a typical EWOD structure. In addition, Fan *et al.*[138] demonstrated DEP-based enrichment of microparticles within an EWOD-driven microdroplet, *via* specially designed DEP actuators between EWOD splitters. Similarly, Nejad *et al.*[139,140] proposed a triangular-shaped DEP trap and performed on-chip enrichment of polystyrene particles.

For LOC applications, Nestor *et al.*[141] used an EWOD–DEP platform to perform 3D cell culture. A GelMA hydrogel precursor, along with suspended cells, is transferred to cell traps, where cells subjected to DEP force are gathered in the round-shaped traps, before the hydrogel is exposed to ultraviolet (UV) for gelation. Komatsu *et al.*[142] implemented EWOD–DEP-based separation of plasma from whole blood. The device uses V_{LF} on the EWOD to draw whole blood from the reservoir, and apply DEP voltage (V_{HF}) on driving electrodes to force blood cells back into the reservoir (Fig. 4G).

Compared to DEP adopted in conventional channel-based microfluidics, EWOD–DEP integrated devices have a remarkable advantage over complexity, for channel-DEP platforms that require control of both passive liquid dispensing and

voltage-based sample handling. However, as DEP and EWOD effects are coupled upon actuation, droplet operation and DEP activation may not be conducted simultaneously, affecting the efficiency and throughput of the sample process in these platforms.

3.3 Acoustic sensing and manipulation

Sensing and actuation using integrated acoustic transducers is a non-contact and efficient approach for biological assays in microfluidic systems. To realize acoustic sensing and actuation, piezoelectric materials are required for the conversion of energy between an electric signal and mechanical vibration. For example, a typical surface acoustic wave (SAW) sensor consists of a piezoelectric substrate, one or more interdigitated transducers (IDTs, or interdigitated electrodes) on the substrate, and a sensing layer.[143] SAWs are excited when AC signals are applied to one of the IDTs, and the waves propagate along the surface of the substrate and can be detected by other IDTs to identify the alterations of physical properties such as the mass of the sensing layer.[144] In contrast to sensing, acoustic transducers may cause droplet motion and are widely implemented in particle manipulation and droplet handling. Therefore, the use of acoustic waves is another potential approach to realize DMF besides EWOD.[145,146]

The combination of acoustic transducers with EWOD is, however, another promising approach to expand the functionality of DMF systems, where acoustic transducers are generally used for sensing and enhancement of droplet manipulation. For combined acoustic sensing, Zhang *et al.*[147,148] integrated a thin-film bulk acoustic wave sensor into a DMF system for a label-free immunoassay in serum. The bulk acoustic wave sensor is fabricated on a silicon-based EWOD bottom plate, including a silicon substrate, a Bragg reflector layer, EWOD electrodes, a piezoelectric layer, and a functionalization layer, where the aluminum nitride (AlN) piezoelectric layer also performs as the dielectric layer for EWOD (Fig. 4H). Direct mass detection can thus be performed as the droplet is positioned on the top of the sensor.

For enhancing droplet manipulation, the introduction of acoustic wave mixers significantly increases the efficiency of mixing compared to EWOD mixing (*i.e.*, moving the merged droplet back and forth). Lu *et al.*[149] used a similar bulk acoustic wave transducer as a micromixer to promote liquid mixing after droplet merging by EWOD. The functionalization layer of the transducer is packaged with an additional SiO_2 layer to prevent contact with the droplets. Madison *et al.*[150] reported the integration of a lead zirconate titanate (PZT) transducer into the top plate of an EWOD device as a micromixer, where a through hole is drilled in the top plate to allow the adhesion of the transducer to the EWOD ground film. Li *et al.*[151,152] demonstrated the integration of SAW with EWOD on lithium niobate ($LiNbO_3$) substrates, where the SAW IDTs are fabricated on the same layer as the EWOD electrodes (Fig. 4I). Particle concentration, acoustic streaming, and mixing are demonstrated using SAWs. Notably, SAWs may afflict damage to the hydrophobic coating of EWOD if the power is too strong, as general hydrophobic fluoropolymers are not strongly adhesive to the dielectric material. Chung *et al.*[153,154] performed acoustic droplet mixing on an EWOD device using an injected air bubble into the droplet. As an acoustic wave applied to the EWOD substrate vibrates the air bubble, the bubble is stimulated and results in microstreaming within the droplet, causing the contents to merge rapidly.

Besides, EWOD was implemented in the tuning of acoustic fields by Bansal *et al.*,[155] where a slit was made in a single plate EWOD device and mounted by a droplet. The structure acts as an active aperture for acoustic wave modulation.

Overall, acoustic waves are efficient tools for both conventional channel-based microfluidics and DMF. Characteristics such as non-contact and efficient are comparable to those of magnetic, optical, and DEP manipulation methods. However, the generation of acoustic waves relies on specialized piezoelectric materials such as PZT, AlN, and $LiNbO_3$, which mainly increases the complexity of the design and fabrication of EWOD devices on the chip scale.

3.4 Integrated sensing

Basic DMF devices, as actuators, possess only the ability to handle liquid. Therefore, an essential step for bringing a digital microfluidic technique into actual LOC applications is integrating detectors into DMF systems. Ranging from the measurement of physical to biochemical signals, these sensors enable integrated sample detection and analysis and have the potential for fully-automatic *in vitro* diagnostic systems for clinical applications. To date, efforts on the chip-scale integration of microsensors on DMF platforms have included mainly droplet position monitoring, electroanalytical measurement, electrochemical analysis, and temperature sensing (see section 2.3 Temperature control). In addition, integrated acoustic transducers are capable of both actuation and sensing, which are introduced in section 3.3.

One of the fundamental purposes for using integrated sensors in DMF devices is droplet position sensing, which allows for feedback control in droplet manipulation and eventually reliable large-scale and high-throughput DMF. To realize a close-looped EWOD-based DMF system, the integration of impedimetric (*i.e.*, capacitance and/or resistance) sensors on individual driving electrodes is a commonly applied method.[156–158] Gong *et al.*[159] first suggested impedance-based sensing for a double-plate EWOD chip. As the dielectric constant differs significantly between droplets (water) and air, the impedance between the device top plate and bottom plate changes significantly at the location of the droplet. Bhattacharjee *et al.*[160] later proposed capacitance sensing between the adjacent electrodes on the bottom plate, acquiring continuous droplet position estimation as the droplet moves between the electrodes. Shih *et al.*[161] implemented capacitance sensing on cell growth monitoring on an EWOD device, where the relationship between impedance and adherent cell density is investigated. Scott-Murrell *et al.*[162] established models for particle-containing EWOD droplet impedance concerning particle size and vertical distribution. Gao *et al.*[163] presented an

intelligent EWOD system in which capacitance-based feedback is enhanced by fuzzy control (Fig. 5A). The system was later implemented in the ion detection of seawater.[164–166] Automated droplet routing experiments were carried out in similar capacitance-based intelligent systems.[18,163] Recently, Perry *et al.*[103,104] demonstrated feedback control over both the liquid volume and the reaction temperature, with both a syringe pump liquid dispenser and a microheater module under PID control for stabilization of droplets during thermal cycles. Additionally, for large-scale TFT-based devices,[13,14] an individual array element (electrode) is composed of separate driving and impedance sensing regions. Compared to small-scale EWOD devices, the large number of electrodes in TFT-based devices allows for digitized sensing of droplets (Fig. 5B). Other approaches for feedback control, such as image-based[167,168] and optic-based,[167,169,170] are also reported.

Integrated electrical sensors in DMF also enable direct and label-free detection of chemical and biological compounds in a sample solution. Choi *et al.*[171] presented an EWOD device with built-in field effect transistors (FETs) for antibody detection. The underlap FET biosensors are positioned at the middle of the driving electrodes, where the dielectric and hydrophobic coating on the drain electrode is removed for direct contact between the antigen coated on the drain electrode and the sample droplets. Drain current is monitored for antibody measurement. Lei *et al.*[172–174] reported a micro-nuclear magnetic resonance (μNMR) technique integrated with the EWOD system, where the EWOD device is combined with a transmitter magnet, an off-chip butterfly coil, and a CMOS transceiver. Avidin concentration is measured in the system by merging biotinylated magnetic particles with sample avidin on EWOD prior to μNMR detection. Mashraei

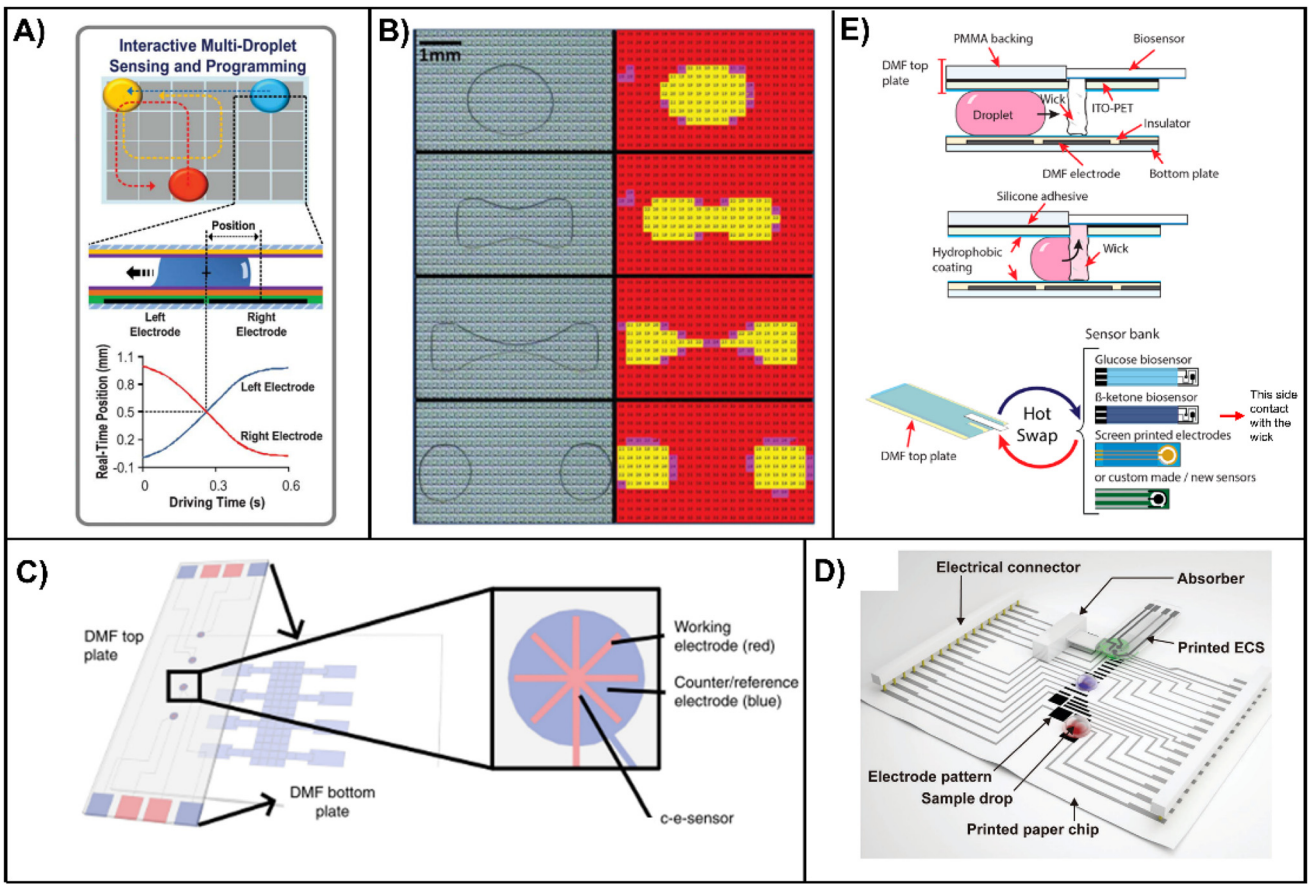

Fig. 5 Integration of sensors on EWOD chips for droplet position monitoring, electrical measurement and electrochemical analyses. (A) An EWOD device with impedance-based multi-droplet sensing and programming. Top: top view of the electrode array and the droplets; middle and bottom: schematic of the impedance-based sensing of real-time droplet positions. Reproduced with permission from ref. 165. Copyright 2019 Elsevier. (B) Photographs (left) and impedance sensor images (right) of an active matrix (thin film transistor array) chip. Droplet location and shape are digitized as each EWOD electrode (colored square) includes an impedance sensor. Reproduced with permission from ref. 13. Copyright 2012, the Royal Society of Chemistry. (C) Schematic of an EWOD device with an integrated electrical sensor on the top plate. c-e sensor: the developed cell-culture/electroanalytical sensor. Reproduced with permission from ref. 176. (D) Conceptual diagram of a paper-based printed EWOD chip for electrochemical analysis. ECS: electrochemical sensor. Reproduced with permission from ref. 16. Copyright 2017 John Wiley and Sons. (E) Schematic of an EWOD device for electrochemical assays with a slot on the top plate for hot-swapping of disposable biosensors. ITO-PET: polyethylene terephthalate films coated with indium-tin oxide, used as the EWOD ground layer, not displayed in the lower diagram. Reproduced with permission from ref. 183. Copyright 2021 American Chemical Society.

et al.[175] demonstrated a fractal capacitance sensor on an EWOD platform for the detection of C-reactive protein. As in many impedance-based droplet position sensing platforms, the specially designed driving electrodes perform both EWOD actuation and capacitance sensing. With immobilized antibodies on the electrode surface, the sensor detects the capacitance shift during the binding of specific proteins. Yu *et al.*[176,177] established an EWOD platform for dopaminergic cell culture and continued dopamine monitoring, which performs voltammetric sensing in the cell culture microwell *via* electrodes on the EWOD top plate etched out of ITO coating (Fig. 5C).

The electrochemical assay is another promising field of application for DMF devices. For integrating a standard three-electrode system for electrochemical detection on the EWOD platform, either the EWOD top plate or the bottom plate needs to be modified. Karuwan *et al.*[178] demonstrated early electrochemical integration on an open EWOD platform with detection wires externally placed on the contact surface. Shamsi *et al.*[179] deposited detector electrodes on the device top plate, while the bottom plate remains a typical EWOD layout. Rackus *et al.*[180] further enhanced the performance of a DMF-based electrochemical assay by replacing conventional planar electrodes with three-dimensionally grown nanostructured microelectrodes (NMEs). Yu *et al.*[181] also used integrated three electrodes and grounding on the EWOD top plate. However, a conflict emerges when the limited lifetime and flexibility of electrochemical sensors are compared with those of DMF, which is a more durable and relatively high-cost platform. To address this issue, Farzbod *et al.*[182] demonstrated EWOD-actuated Ag/AgCl electrode fabrication *via* electroplating and chemical oxidation, extending the lifetime of the integrated device. Ruecha *et al.*[16] fabricated paper-based printed EWOD chips with replaceable electrochemical sensor modules positioned on top of the droplets (Fig. 5D). De Campos *et al.*[183] presented an interface between the EWOD platform and commercial electrochemical sensor strips, where a 1 mm × 1 mm KimWipe tissue wick is used to absorb the dispensed sample and deliver it to the biosensor plugged at the back of the EWOD top plate, allowing for a rapid switch for the desired biosensor in ongoing assays (Fig. 5E).

4. Hybrid actuation

A digital microfluidic device provides accurate and programmable manipulation over an individual droplet, making the droplet appropriate for sequential biochemical reactions, but the device is limited to a small volume of samples and reagents. In contrast, conventional channel-based droplet microfluidics is well-suited for high-throughput sample treatment and flow-based analyses. A combination of both active and passive actuation approaches on a single chip is originally referred to as "hybrid microfluidics", where the active (digital) manipulation either runs separately and interfaces with pump-driven microchannels (passive) or serves as a supplementary control in channel-based systems.

With hybrid actuation approaches, microfluidic systems may possess both the ability of efficient batch treatment and more sophisticated individual control, which further enhances the integration and automation level for existing LOC systems.

4.1 Digital-channel interfacing

To utilize the advantages of both systems of DMF and channel-based microfluidics, a significant approach is connecting the two distinct systems with interfaces, where DMF is used for either sample pretreatment or downstream analyses.

Digital-to-channel interfacing allows for integrated digital sample pretreatment and channel-based downstream analysis. To interface with DMF chips, microfluidic channels are positioned either on the same surface as the DMF bottom plate (horizontal layout) or beneath the DMF layer (vertical layout). Abdelgawad *et al.*[184] presented the first interface between a single plate EWOD and a PDMS channel on a shared substrate, where the open EWOD platform performs droplet merging and transportation into the channel. Such a side-on interface is facile yet may cause dispensing errors and evaporation problems. Watson *et al.*[185] improved this method by placing EWOD actuators and microchannels in vertically stacked substrates and created a multilayered hybrid device, enabling interfacing of the top double plate (enclosed) EWOD substrates with the bottom substrate of microchannels, thus allowing for accurate droplet dispensing and reduced evaporation (Fig. 6A). Abadian *et al.*[186] illustrated an interface between EWOD and a microfluidic paper-based analytical device (μPAD). This filter paper-based device uses a paper-folding style to create a contact between the μPAD and screen-printed electrodes, where droplets transported by the electrodes are adsorbed onto the μPAD *via* capillary force. Gach *et al.*[102] demonstrated the potential of a digital-channel hybrid device in complex biomedical assays, by establishing an automated microfluidic system for on-chip gene editing for bacteria and fungi such as *E. coli* and yeast (Fig. 6B). The system includes EWOD-based heat-shock cell transformation and subsequent channel-based cell culture and screening. The oil phase is continuously induced from the digital-channel interface to prevent evaporation, allowing for cell culture for up to 5 days. Recently, Sathyanarayanan *et al.*[17] demonstrated another digital-to-channel chip for microchip electrophoresis, where non-cleanroom techniques are used throughout device fabrication (Fig. 6C).

In contrast, the channel-to-digital interface considers channel-based sample preparation prior to DMF-based manipulation. Wu *et al.*[187] reported an EWOD sample treatment platform with capillary inlets and outlets. A channel-based electrical cell lysis chip transfers the cell lysate into the platform *via* capillary tubes. In order to process the incoming samples, the EWOD chip converts the continuous phase from the capillaries into droplets. Shih *et al.*[188] developed a droplet-to-digital hybrid microfluidic device for single cell analysis. In this device, single cells are encapsulated in droplets by a flow-

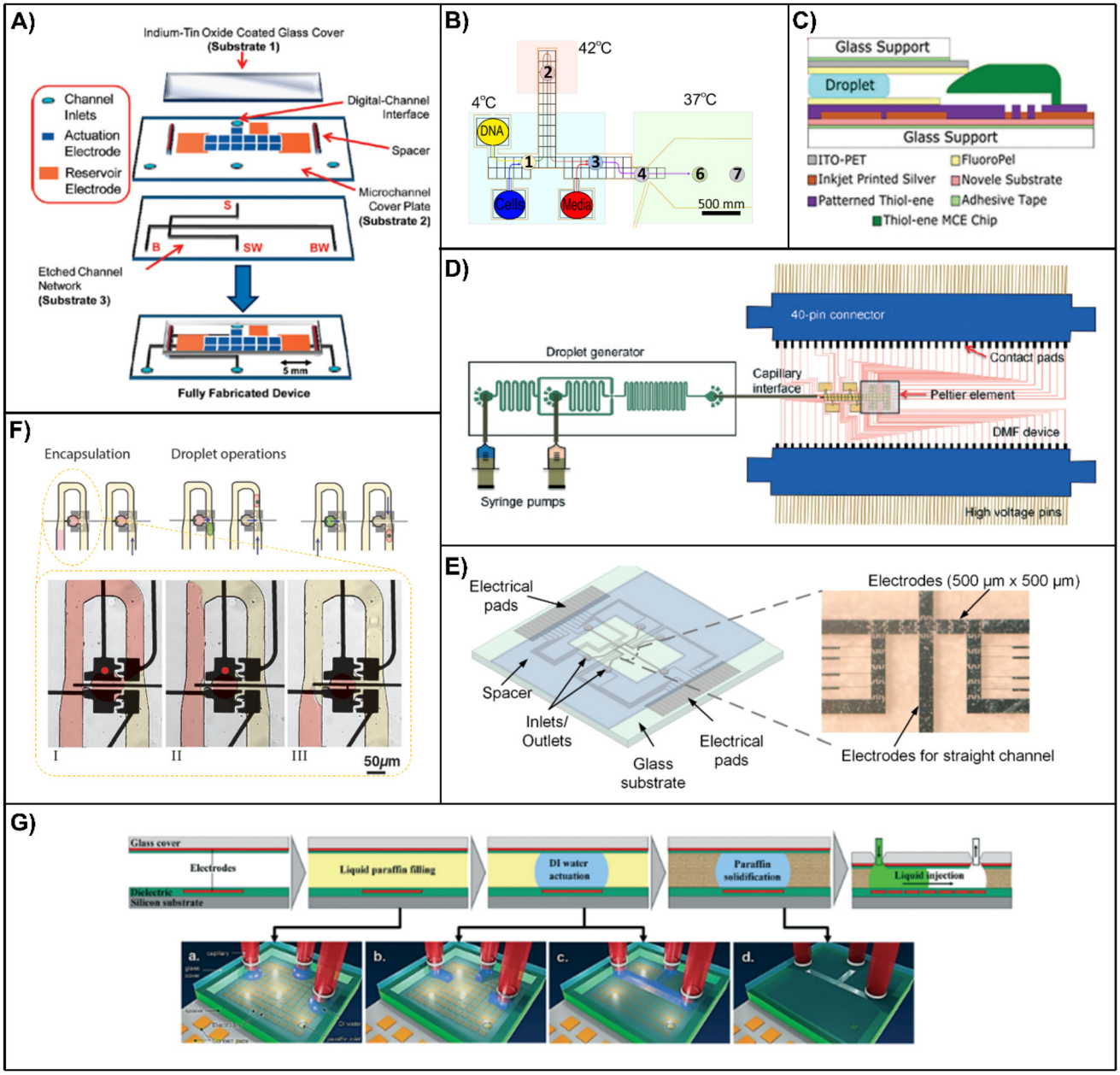

Fig. 6 Digital-channel interfacing and EWOD-assisted devices. (A) Schematic of a digital-to-channel device with a vertical interface, where holes on the DMF bottom plate connect DMF with the flow channels on a glass substrate. Reproduced with permission from ref. 185. Copyright 2010 American Chemical Society. (B) Schematic diagram of a digital-to-channel device for gene editing of bacteria and subsequent encapsulation and culture. Numbers 1–7 refer to the chip-based process of bacterial gene editing. The digital-to-channel interface is introduced at the entrance of the 37 °C culture region. Reproduced with permission from ref. 102. Copyright 2016 American Chemical Society. (C) Schematic of a digital-to-channel device with a horizontal interface connecting the EWOD with a capillary chip for electrophoretic analysis. MCE: microchip capillary electrophoresis; HV: applied voltage for MCE; FluoroPel: a hydrophobic coating. Reproduced with permission from ref. 17. (D) Schematic of a channel-to-digital device for single cell encapsulation and processing in which the droplets formed in the channel device on the left are transferred to the DMF device on the right. Reproduced with permission from ref. 188. Copyright 2015, the Royal Society of Chemistry. (E) Schematic and the photograph of a hybrid device with a straight channel electrode for washing of magnetic particles with syringe pumps (not shown). Reproduced with permission from ref. 52. (F) Workflow of a channel-based hybrid chip for on-demand cell trapping and droplet generation. Top: schematic diagram of the single cell trapping bypass structure enhanced with EWOD electrodes and the working process; bottom (I–III): photographs of the EWOD-assisted droplet generation at the bypass structure; red dots indicate active electrodes. Reproduced with permission from ref. 190. Copyright 2020 John Wiley and Sons. (G) Re-routing protocol of a channel-based chip under EWOD and LDEP effects. Reproduced with permission from ref. 191. Copyright 2013, the Royal Society of Chemistry.

focusing droplet generation chip, and the droplets are subsequently transferred to the EWOD platform *via* a capillary interface (Fig. 6D). The electrodes at the interface are suited for transferring individual cell-containing droplets onto the assay zones of the EWOD platform, where single cells are cultured with a gradient ionic liquid for toxicity screening. Another similar device by Shih *et al.*[106] is used for DNA synthesis.

4.2 Electrowetting-assisted channel microfluidics

The principle of active actuation may also be used as a complementary approach for channel-based droplet microfluidic systems to enhance droplet generation and manipulation. Devices may be built upon established DMF substrates where fluidic channels are patterned above the actuators, allowing for "digital" enhancement in the control of the continuous or two-phase flow.[52,58]

Gu *et al.*[189] established a polydimethylsiloxane (PDMS) imprinting fabrication process for an EWOD-channel hybrid microfluidic device, in which EWOD top and bottom plates are fabricated using a standard cleanroom procedure on an ITO glass substrate, and the UV-curable gel Norland Optical Adhesive (NOA) 81 is coated on a Teflon AF surface and imprinted by a PDMS mold with channel structures. The adhesion between NOA and Teflon AF proved sufficient to bond and seal the channels on the EWOD substrate. An EWOD-assisted flow-focusing droplet generation test was carried out using this technique.

For biomedical applications, Liu *et al.*[52] developed an EWOD-channel combined chip for particle-based immunoassays, where a virtual fluidic channel (straight channel) is present for the efficient washing of MPs (Fig. 6E). This virtual channel is realized *via* a rectangular EWOD electrode, whereas a syringe pump is introduced to drive the wash buffer through the virtual channel while an EWOD voltage is applied to the channel electrode. Samlali *et al.*[190] demonstrated an on-demand droplet generation device for single cell encapsulation. By applying PDMS microchannels directly onto the dielectric layer of the EWOD substrate, the authors first performed single cell trapping *via* microchannels in a continuous water phase, and then completed single cell encapsulation (*i.e.*, droplet splitting) *via* the EWOD electrodes located underneath the channel trap (Fig. 6F). Additionally, the on-demand EWOD-assisted droplet generation method decouples the droplet size from the input flow rate, providing an extra degree of freedom of liquid handling within the device.

Renaudot *et al.*[191] presented a reconfigurable microfluidic platform for continuous flow. Built on a double plate EWOD, the chip manipulates the water phase to fill a continued space between two liquid inlets, while the remaining gap is filled with liquid paraffin wax, which is water-insoluble and may solidify and form a substantial sidewall of flow channels around the patterned water phase at a low temperature. The pattern of the channels could thus be readjusted at will by forming the water phase with EWOD (Fig. 6G). Another distinct application for DMF in conventional microfluidic platforms is the active valve. Ahamed *et al.*[192] developed a hybrid device where a channel flow is controlled by an EWOD-driven valve. A thermo-responsive polymer performs as the core component of the valve, which normally blocks the channel flow and liquefies at high temperatures, thus allowing EWOD displacement.

5. Biomedical applications

5.1 Immunoassay

One of the priorities of LOC systems is achieving rapid and sensitive detection of disease-related biomarkers (antigens) for clinical diagnosis, based on the binding of the antigens by antibodies in immunoassays. Therefore, immunoassays provide an effective tool for both quantitative and qualitative detection of biomarkers with high specificity *via* antibody–antigen binding. Commonly, immunoassays are based on radioimmunoassay (RIA) and enzyme-linked immunosorbent assay (ELISA),[193] where the binding of the antibody with the target antigen is monitored with either radioactivity or enzymatic reactions. In addition, an immunoassay may utilize direct colorimetric, fluorescence, chemiluminescence, and other methods. A conventional protocol for an immunoassay performed in clinical laboratories usually includes multiple labeling, binding, and washing steps, which are applicable for an EWOD system toward the development of a fully automated procedure.

An integrated magnetic control unit provides EWOD with the ability to aggregate and thus washing of MPs, enabling a full particle (bead)-based immunoassay procedure on an EWOD chip. For instance, Ng *et al.*[46] developed an on-chip ELISA protocol on thyroid stimulating hormone and 17β-estradiol samples using antibody-coated MPs, where the assay volume is reduced by 10-fold (2.4 μL) compared to traditional well-plate ELISA with comparable sensitivity. Accordingly, the total assay time is significantly reduced. Liu *et al.*[52] also realized MP-based ELISA on human interleukin-6 samples on a virtual channel EWOD device. Jin *et al.*[50] performed a chemiluminescence immunoassay on B-type natriuretic peptide samples. Guo *et al.*[64] demonstrated the feasibility of an MP-based protein–aptamer system (human EpCAM and aptamer SYL3C) on an integrated EWOD platform, and they also developed an antigen–antibody system (H5N1), where the antigen bound to MPs is incubated with an antibody solution and washed for measurement. Ng *et al.*[194] used an integrated DMF system to perform MP-based ELISA for measles and rubella testing. This system was packaged and underwent field validations to demonstrate its potential for point-of-care diagnosis.

Under specific circumstances, such as blood typing, immunoassays may also be performed on DMF systems without the need for labeling and washing (and hence the MPs). In blood typing, hemagglutination caused by the addition of blood-typing antibodies is clearly distinguishable with optical instruments. Sklavounos *et al.*[195] used a combined DMF system for hemagglutination assays, where lyophilized

assay reagents (anti-A, anti-B, anti-A, B, and anti-RhD antibodies) are preloaded into the DMF cartridge and dissolved with water before adding the whole-blood sample. The sample is then dispensed and mixed with the antibodies for the agglutination test. The test results are monitored through a camera above the DMF cartridge and assessed using an automated image analysis program.

In addition to the automated handling of fluids and antibody-bound MPs, the use of an appropriate temperature is also essential to improve the binding efficiency of antibodies and thus the sensitivity of the assay. Shen *et al.*[100] performed an immunosorbent assay on three acute myocardial infarction biomarkers from a patient's blood samples, in which the temperature is maintained at 37 °C as measured using an integrated thermocouple, reducing the time required for saturation. Sista *et al.*[31] reported an EWOD system with cell lysis, plasma preparation, MP washing, thermocycling, and incubation functionalities, enabling an on-chip immunoassay, a chemical/enzymatic assay, and PCR. The advantage of the minimal sample requirement of the system makes it appropriate for diagnosis in newborns.

To date, most reported works on EWOD-based immunoassays rely on MPs as a substrate for antibody-binding reactions. As an LOC immunoassay emerges as an effective approach for point-of-care diagnosis, the EWOD platform possesses the following advantages: (1) miniaturization, which reduces the reaction volume of the assay to the sub-microliter scale and requires a smaller amount of rare sample, less-costly reagents (*e.g.*, antibodies) and a shorter assay time; (2) automation and repeatability, which alleviates biases among operators and extensive labor. The combination of magnetic and thermal components with DMF plays a crucial role in achieving an EWOD-based immunoassay. However, adsorption of proteins onto the EWOD surface (biofouling) is an inevitable issue, especially in protein-related studies.

5.2 Nucleic acid testing

Nucleic acid testing (NAT) is another vital part of both molecular biology studies and clinical diagnosis. Prior to most detection methods on nucleic acids, an extraction step is required to release DNA or RNA molecules from the raw sample and remove inhibitory substances, including DNase and RNase, that are inhibitors of subsequent detection. Traditional extraction methods consist of chemical and solid-phase methods, including phenol–chloroform extraction, chromatography, and bead-based electrostatic adsorption.[196] Bead-based adsorption is compatible with automated analyzers. Similarly, integrated EWOD with MP aggregation ability is also well-suited for automated nucleic acid extraction. Chiang *et al.*[54,55] extracted cell-free DNA from a mouse embryo culture medium using MP adsorption, indicating that a conventional bead-based DNA extraction protocol is compatible with the EWOD platform. The extraction efficiency is then evaluated *via* qPCR. Hung *et al.*[56] demonstrated EWOD bead-based genomic DNA extraction, which also includes manipulation of whole blood and on-chip cell lysis steps.

PCR is a traditional method that is one of the most accepted technologies for nucleic acid detection.[197] This technology utilizes heat-resistive Taq DNA polymerase and specially designed primer sequences to exponentially amplify (replicate) the desired DNA sequence, through a series of denaturing–annealing (typically 95 °C–60 °C) thermal cycles. The detection after amplification is either done by gel electrophoresis (qualitative) after all cycles, or during each thermal cycle by an optical method with the addition of a fluorescent dye or a probe sequence (*i.e.*, qPCR, semi-quantitative). EWOD-based PCR has undergone extensive research, where the strategy of thermal cycling is divided into a stationary droplet and a shuttling droplet, as detailed in section 2.3. When integrating qPCR on the platform, an optical system with fluorescence excitation and detection is also required. Recent research on EWOD-based PCR focuses on the integration of third-generation PCR (*i.e.*, digital PCR, dPCR) on EWOD, which allows for ultra-sensitive detection and quantification of the desired sequence.[26]

Amplification of the target DNA sequence is essential for the sensitivity of the assay. Isothermal amplification technologies are developed as alternatives to PCR, where a constant temperature is maintained for DNA amplification cycles, thus requiring less complexity for external temperature control devices.[198] Both separate and integrated heater configurations are observed for EWOD-based isothermal amplification (see Table 1). Typically, Narahari *et al.*[33] realized portable detection of Zika viral RNA *via* nucleic acid sequence based amplification (NASBA) from spiked plasma samples with integrated bead-based RNA extraction. The amplification step includes 2-minute annealing at 65 °C, 10-minute cooling at 41 °C, manual addition of an enzyme mix, and subsequent amplification at 41 °C for 1.5 h. An endpoint colorimetric assay is then used as a qualitative evaluation, as the system does not include real-time optical devices and procedures. Wan *et al.*[99] performed a LAMP assay on DNA samples of a blood parasite, *T. brucei*, on a handheld EWOD system, where the temperature was maintained at 65 °C during the assay. SYBR Green dye was added *via* EWOD after the amplification step for endpoint analysis. Coelho *et al.*[95] combined EWOD-based LAMP with standard fluorescence microscopy for real-time analysis. Kalsi *et al.*[14] demonstrated a real-time RPA assay on bacterial DNA using a TFT-based EWOD device, where the integrated heater maintained a temperature of 39 °C during the assay.

Apart from its significance in biological research, DNA sequencing is another important method for the detection of genetic and epigenetic biomarkers in NAT.[199,200] The flexible sample dispensing, mixing, and splitting capabilities of EWOD provide a feasible solution to automated sample preparation. When combined with MP control, the platform is fit for a standard pyrosequencing protocol for DNA methylation detection.[34,58] For example, Ruan *et al.*[59] performed a full on-chip pyrosequencing protocol where MPs are used to retain sample DNA sequences, while enzymes, dNTPs, and other essentials are mixed consecutively with the MP suspension. Chemiluminescence signals are collected *via* an integrated

Table 1 Summary of the combination forms of EWOD and their applications

Combination form	Application	Ref.
MP[a] control unit	Cell capture	44 and 45
	Particle-based immunoassay	31, 46–52, 63 and 64
	Nucleic acid extraction	33 and 54–56
	Sequencing	34, 57 and 59
	Improved MP collection efficiency	50, 60 and 62–64
Discrete OEW[b]	Basic droplet manipulation	66, 74 and 75
Continuous OEW	Basic droplet manipulation	67–69, 72 and 76
OT[c]	Cell/particle sorting	80 and 81
OET[d]	Cell/particle manipulation	83–86
Laser	Cell lysis	12
Separate heater	Cell culture/processing	87, 102 and 103
	PCR[e]	35, 36, 44, 88 and 115
	Isothermal amplification	33 and 97–99
	Other NAT[f]	101, 104 and 106
	Immunoassay/enzymatic reactions	100 and 105
Integrated/multifunctional heater	PCR	89–94, 107 and 108
	Isothermal amplification	14, 95 and 96
	Other NAT	57 and 109
	Molecular synthesis	110 and 111
	Mass spectrometry	114
	Others	112
Surface modification	Cell culture/adhesion and further assay	11, 12, 120 and 121
	Single-cell/particle trapping	122 and 123
	Droplet generation	101
	Mass spectrometry	114 and 211
Surface microstructure	Droplet retention	128
	Single-cell/particle trapping	125–127
	3D cell culture	124, 129
	Mass spectrometry	130, 131, 206 and 210
DEP[g]	Particle enrichment	137–140
	Cell trapping	141
	Plasma separation	142
Acoustic waves	Immunoassay	147
Integrated sensor	Droplet position feedback	13, 14, 18, 156–165 and 167–170
	Monitoring of biomolecules	171 and 175–177
	Miniaturized NMR[h]	172–174
	Electrochemical assay	16 and 178–183
Digital-channel interface	Basic droplet manipulation	184–186
	Capillary electrophoresis	17
	Cell culture and processing	102
Channel-digital interface	Sample replenishment	187
	Cell encapsulation	188
	DNA assembly	106
EWOD[i]-assisted channel	Valving	189 and 192
	Channel reconfiguration	191
	Immunoassay	52
	Cell encapsulation	190

[a] Magnetic particle. [b] Optoelectrowetting. [c] Optical tweezer. [d] Optoelectronic tweezer. [e] Polymerase chain reaction. [f] Nucleic acid testing. [g] Dielectrophoresis. [h] Nuclear magnetic resonance. [i] Electrowetting-on-dielectric.

photomultiplier tube (PMT) for methylation analysis. In addition, single-cell level sequencing is also feasible on integrated EWOD platforms, provided that cells are trapped prior to preparation protocols.[122,127]

5.3 Cell-based studies

In vitro cell culture techniques have been developed as early as 1910s.[201] Cell models, in parallel with animal models, provide an effective approach for both physiological and pathological studies, as well as drug assessments. To date, EWOD-based cell studies have covered various types of cell models, including suspension cells, 2D adherent cells, 3D spheroids (and organoids), and single-cell analyses, which have also been comprehensively summarized in previous reviews by Pang *et al.*[28,202]

Advances in recent years (since 2020) focus mainly on single-cell studies, where integrated systems provide extra control over individual cells dispensed on the EWOD chips. To achieve single cell identification, isolation, and subsequent manipulation, Xu *et al.*[122] and Ruan *et al.*[127] used a microstructure on the chip surface and the dynamic characteristics of EWOD-driven droplets to ensure that only a single cell from the suspension is trapped in the desired location, while the remaining cells are removed through washing. Similarly, Samlali *et al.*[190] introduced microwells and channel flow to realize single cell entrapment, whereas EWOD performs to

split the continuous liquid phase to achieve single cell isolation. These methods, however, are not selective to individual cells and hence inconvenient for heterogeneity studies in a cell population. Lamanna *et al.*[12] relied on image-based algorithms to locate specific cells from an adherent culture, and used a laser beam to selectively lyse desired cell targets, supporting further single cell genomic, transcriptomic, and proteomic analyses. Kumar *et al.*[81] combined optical tweezers with an EWOD platform to perform single MP manipulation for bacterial detection, where the laser beam supports selective transportation of an individual MP loaded with bacteria within an EWOD droplet. Instead of picking out each individual cell for further study, Zhai *et al.*[125] developed a 30 × 30 microwell array to compartmentalize up to 20% of cancer cells for a drug toxicity test on an EWOD surface. After dispensing of cells and the drug on the EWOD chip, it is transferred to an incubator for about 24 h, and then, cell viability is observed for evaluation.

5.4 Mass spectrometry

Mass spectrometry (MS) is a powerful tool for chemical and biological studies. For biomedical applications, MS is commonly used for diagnosis and proteomic and genomic studies, which includes a prolonged process for sample preparation. EWOD provides an alternative to the laborious conventional pretreatment process for MS, improving the efficiency of MS and reducing its consumption of samples. The combination of EWOD with MS has been thoroughly discussed in a previous review by Kirby and Wheeler,[203] in which the authors divided the application of EWOD–MS systems into off-line and in-line analyses, depending on whether the EWOD remains operational during the MS analysis.

To date, the most commonly studied MS integrated with EWOD has been realized *via* matrix-assisted laser desorption/ionization (MALDI) or electrospray ionization (ESI). For EWOD-MALDI-MS, one of the first protocols developed by Wheeler *et al.*[204,205] includes dispensing of the sample protein, drying, rinsing, and addition of the MALDI matrix, before removing the device top plate (*i.e.*, off-line) and placing the bottom plate onto a MALDI target plate. This protocol was later enhanced by Nelson *et al.*[114] with localized temperature control and hydrophilic sites to accelerate the trypsin digestion rate of proteins, sample drying, and matrix crystallization. The strategy of a multifunctioning actuator/heater was implemented to avoid extra complexity in the system, as the sample droplet will remain anchored during the drying and crystallization process. Similarly, Lapierre *et al.*[206,207] developed matrix-free surface-assisted laser desorption–ionization (SALDI) MS on a silicon-based EWOD substrate, on which silicon nanowires are patterned as an alternative to the MALDI matrix for MS analysis. Jang *et al.*[208] demonstrated a paper-based EWOD device for protein digestion prior to MALDI-MS. Kudina *et al.*[209,210] developed an "e-MALDI" method integrating interdigitated EWOD electrodes with the MALDI target plate, where the AC actuation signal applied to the sample droplet results in a shrinking contact line during the drying and crystallization process, eliminating the "coffee stain" pattern in conventional MALDI sample preparation. Ruan *et al.*[211] combined EWOD-based single cell (circulating tumor cell) isolation with MALDI-MS analysis. Gene mutation information of the circulating tumor cells is identified *via* the inherent mass differences of the DNA sequences.

For EWOD-ESI-MS, the spraying ionization process is either performed in an external emitter while the sample droplets in the EWOD chip are transferred to the emitter *via* capillary tubes, or realized *via* a specialized microstructure on the EWOD substrates. Both approaches enable in-line MS analysis. Baker and Roper[212] established an eductor for coupling EWOD sample preparation with ESI-MS. A transfer capillary, an ESI needle, and a gas nozzle allow the transfer of the sample from EWOD for electrospray ionization. Hu *et al.*[213] used a similar strategy to couple EWOD actuation with Venturi easy ambient sonic-spray ionization (V-EASI). Kirby and Wheeler[131] developed a "microfluidic origami" device (Fig. 4F) on a flexible EWOD substrate which is folded into a conical shape for electrospray. The sample droplet is transferred by EWOD to the apex of the cone, where an electrospray voltage is applied and results in the generation of a Taylor cone through the apex. Das *et al.*[130] developed an "on-the-fly" ESI-MS on an EWOD platform (Fig. 4E). The spraying is directly performed by applying a pulsed high voltage through a micro-hole in the EWOD top plate. A significant advantage of such in-line analyses is the ability to conduct real-time MS measurement on the sample, as well as subsequent operation on EWOD.

6. Conclusion and perspectives

The increasing need for efficient, portable, reliable lab-on-a-chip systems for both biomedical research and clinical prognosis has called for a variety of technical approaches, among which EWOD-based DMF presented unparalleled flexibility and simplicity in liquid manipulation capabilities. Based on the existing EWOD platforms, efforts on the integration and combination of different microfluidic sensor and actuator systems have largely expanded the functionalities of DMF towards more specialized and practical use.

To date, three major categories of combined EWOD systems have been reported in the literature with their distinct purposes and features. System-level integration allows for external magnetic and optical forces and temperature control ability to be added to EWOD systems, which are generally non-contact and require minimal modifications to the existing system; chip-scale integrated sensors, actuators, and microstructures improve EWOD platforms by various means; hybrid systems with both EWOD and pumping actuators and/or microchannels combine the advantages of both passive batch treatments in flow channels and flexible maneuvering on EWOD actuators.

As combined EWOD-based DMF systems continue to evolve, more powerful functionalities and sophisticated controls are being merged with the adaptable EWOD technique

towards practical "sample in, result out" LOC systems. In addition to improved sensitivity and specificity and shortened time demanded by general microfluidic LOC platforms, these systems also face challenges from the following aspects: (1) *Consumable cost*: as a disposable chip (cartridge) is a design necessary for nearly all microfluidic LOC systems, the current DMF consumables are significantly more costly due to their electrode patterning, dielectric and hydrophobic treatment, which is more costly in TFT-based and chip-scale integrated devices; (2) *Intelligence*: the current combined DMF systems are complicated and have an excess degree of freedom when conducting predetermined droplet actions, hence it is crucial to fully develop the potential of the DMF system with respect to its efficiency, throughput and robustness using intelligent software including the functionalities of automated droplet routing, sample identification and troubleshooting; and (3) *Complexity*: the introduction of integrated sub-systems results in increased complexity in both fabrication and usage, thus the compatibility and tuning of basic EWOD with additional sensors/actuators should been taken into consideration for fabricating and using these systems. Accordingly, future combined EWOD-based DMF systems may take measures to address the abovementioned issues. For the cost issue, two possible approaches may be adopted, *i.e.*, either focus on low-cost substrates and fabrication processes, or remove costly components (electrode arrays, sensors) from the disposable parts. For the intelligence issue, automated droplet routing and sample identification/operation can be achieved *via* an optically or electrically close-looped system and the introduction of machine learning algorithms for specified cases, towards an autonomous droplet microprocessor and analyzer for highly efficient biomedical analyses.

Conflicts of interest

There are no conflicts of interest to declare.

Acknowledgements

This work is supported by grants from National Natural Science Foundation of China (no. 62231025, 61971410 and 82170110), Shanghai Municipal Science and Technology Major Project (no. ZD2021CY001), Shanghai Sailing Program (no. 20YF1457100), Shanghai Engineer & Technology Research Center of Internet of Things for Respiratory Medicine (20DZ2254400) and Shanghai Key Laboratory of Lung Inflammation and Injury (20DZ2261200).

References

1 K. Choi, A. H. C. Ng, R. Fobel and A. R. Wheeler, in *Annual Review of Analytical Chemistry*, ed. R. G. Cooks and E. S. Yeung, 2012, vol. 5, pp. 413–440.
2 T. S. Kaminski and P. Garstecki, *Chem. Soc. Rev.*, 2017, **46**, 6210–6226.
3 W. C. Nelson and C. J. Kim, *J. Adhes. Sci. Technol.*, 2012, **26**, 1747–1771.
4 A. R. Wheeler, *Science*, 2008, **322**, 539–540.
5 S. K. Fan and F. M. Wang, *Lab Chip*, 2014, **14**, 2728–2738.
6 H. Cheng, H. Liu, W. Li and M. Li, *Electrophoresis*, 2021, **42**(21–22), 2329–2346.
7 D. Baigl, *Lab Chip*, 2012, **12**, 3637–3653.
8 S. P. Zhang, J. Lata, C. Chen, J. Mai, F. Guo, Z. Tian, L. Ren, Z. Mao, P.-H. Huang, P. Li, S. Yang and T. J. Huang, *Nat. Commun.*, 2018, **9**, 2928.
9 J. Li, N. S. Ha, T. Liu, R. M. van Dam and C. J. Kim, *Nature*, 2019, **572**, 507–510.
10 R. W. Barber and D. R. Emerson, in *Microdroplet Technology: Principles and Emerging Applications in Biology and Chemistry*, ed. P. Day, A. Manz and Y. Zhang, Springer New York, New York, NY, 2012, pp. 77–116, DOI: **10.1007/978-1-4614-3265-4_4**.
11 I. A. Eydelnant, U. Uddayasankar, B. B. Li, M. W. Liao and A. R. Wheeler, *Lab Chip*, 2012, **12**, 750–757.
12 J. Lamanna, E. Y. Scott, H. S. Edwards, M. D. Chamberlain, M. D. M. Dryden, J. Peng, B. Mair, A. Lee, C. Chan, A. A. Sklavounos, A. Heffernan, F. Abbas, C. Lam, M. E. Olson, J. Moffat and A. R. Wheeler, *Nat. Commun.*, 2020, **11**, 5632.
13 B. Hadwen, G. R. Broder, D. Morganti, A. Jacobs, C. Brown, J. R. Hector, Y. Kubota and H. Morgan, *Lab Chip*, 2012, **12**, 3305–3313.
14 S. Kalsi, M. Valiadi, M. N. Tsaloglou, L. Parry-Jones, A. Jacobs, R. Watson, C. Turner, R. Amos, B. Hadwen, J. Buse, C. Brown, M. Sutton and H. Morgan, *Lab Chip*, 2015, **15**, 3065–3075.
15 Z. J. Luo, J. Z. Xu, Z. Y. Pan, H. Yin, L. Cao, G. F. Zhou and S. Y. Liu, *IEEE Access*, 2022, **10**, 30573–30582.
16 N. Ruecha, J. Lee, H. Chae, H. Cheong, V. Soum, P. Preechakasedkit, O. Chailapakul, G. Tanev, J. Madsen, N. Rodthongkum, O. S. Kwon and K. Shin, *Adv. Mater. Technol.*, 2017, **2**, 1600267.
17 G. Sathyanarayanan, M. Haapala, C. Dixon, A. R. Wheeler and T. M. Sikanen, *Adv. Mater. Technol.*, 2020, **5**, 2100491.
18 C. Q. Li, K. D. Zhang, X. B. Wang, J. Zhang, H. Liu and J. Zhou, *Sens. Actuators, B*, 2018, **255**, 3616–3622.
19 K. D. Zhang, W. Wang, C. Q. Li, A. Riaud and J. Zhou, *AIP Adv.*, 2020, **10**, 055227.
20 G. Bindiganavale, S. M. You and H. Moon, Study of hotspot cooling using electrowetting on dielectric digital microfluidic system, 27th IEEE International Conference on Micro Electro Mechanical Systems (MEMS), San Francisco, CA, 2014.
21 P. Y. Paik, V. K. Pamula and K. Chakrabarty, *IEEE Trans. Very Large Scale Integr. Syst.*, 2008, **16**, 432–443.
22 B. Berge and J. Peseux, *Eur. Phys. J. E: Soft Matter Biol. Phys.*, 2000, **3**, 159–163.
23 L. Dong, A. K. Agarwal, D. J. Beebe and H. R. Jiang, *Nature*, 2006, **442**, 551–554.

24 S. Kuiper and B. H. W. Hendriks, *Appl. Phys. Lett.*, 2004, **85**, 1128–1130.
25 S. K. Vashist, P. B. Luppa, L. Y. Yeo, A. Ozcan and J. H. T. Luong, *Trends Biotechnol.*, 2015, **33**, 692–705.
26 X. Rui, S. Song, W. Wang and J. Zhou, *Biomicrofluidics*, 2020, **14**, 061503.
27 A. H. C. Ng, B. B. Li, M. D. Chamberlain and A. R. Wheeler, in *Annual Review of Biomedical Engineering*, ed. M. L. Yarmush, 2015, vol. 17, pp. 91–112.
28 L. Pang, J. Ding, X.-X. Liu and S.-K. Fan, *TrAC, Trends Anal. Chem.*, 2019, **117**, 291–299.
29 J. Li and C. J. Kim, *Lab Chip*, 2020, **20**, 1705–1712.
30 R. Sista, Z. S. Hua, P. Thwar, A. Sudarsan, V. Srinivasan, A. Eckhardt, M. Pollack and V. Pamula, *Lab Chip*, 2008, **8**, 2091–2104.
31 R. S. Sista, R. Ng, M. Nuffer, M. Basmajian, J. Coyne, J. Elderbroom, D. Hull, K. Kay, M. Krishnamurthy, C. Roberts, D. Wu, A. D. Kennedy, R. Singh, V. Srinivasan and V. K. Pamula, *Diagnostics*, 2020, **10**, 21.
32 S. Lin, Y. Liu, M. Zhang, X. Xu, Y. Chen, H. Zhang and C. Yang, *Lab Chip*, 2021, **21**, 3829–3849.
33 T. Narahari, J. Dahmer, A. Sklavounos, T. Kim, M. Satkauskas, I. Clotea, M. Ho, J. Lamanna, C. Dixon, D. G. Rackus, S. J. R. da Silva, L. Pena, K. Pardee and A. R. Wheeler, *Lab Chip*, 2022, **22**, 1748–1763.
34 D. J. Boles, J. L. Benton, G. J. Siew, M. H. Levy, P. K. Thwar, M. A. Sandahl, J. L. Rouse, L. C. Perkins, A. P. Sudarsan, R. Jalili, V. K. Pamula, V. Srinivasarn, R. B. Fair, P. B. Griffin, A. E. Eckhardt and M. G. Pollack, *Anal. Chem.*, 2011, **83**, 8439–8447.
35 Z. S. Hua, J. L. Rouse, A. E. Eckhardt, V. Srinivasan, V. K. Pamula, W. A. Schell, J. L. Benton, T. G. Mitchell and M. G. Pollack, *Anal. Chem.*, 2010, **82**, 2310–2316.
36 E. Wulff-Burchfield, W. A. Schell, A. E. Eckhardt, M. G. Pollack, Z. S. Hua, J. L. Rouse, V. K. Pamula, V. Srinivasan, J. L. Benton, B. D. Alexander, D. A. Wilfret, M. Kraft, C. B. Cairns, J. R. Perfect and T. G. Mitchell, *Diagn. Microbiol. Infect. Dis.*, 2010, **67**, 22–29.
37 A. K. Gupta and M. Gupta, *Biomaterials*, 2005, **26**, 3995–4021.
38 P. Dunne, T. Adachi, A. A. Dev, A. Sorrenti, L. Giacchetti, A. Bonnin, C. Bourdon, P. H. Mangin, J. M. D. Coey, B. Doudin and T. M. Hermans, *Nature*, 2020, **581**, 58–62.
39 Y. Fouillet, D. Jary, C. Chabrol, P. Claustre and C. Peponnet, *Microfluid. Nanofluid.*, 2008, **4**, 159–165.
40 G. J. Shah, E. Pierstorff, D. Ho and C. J. C. Kim, Meniscus-assisted magnetic bead trapping on EWOD-based digital microfluidics for specific protein localization, 14th International Conference on Solid-State Sensors, Actuators and Microsystems/21st European Conference on Solid-State Transducers, Lyon, FRANCE, 2007.
41 Y. Wang, Y. Zhao and S. K. Cho, *J. Micromech. Microeng.*, 2007, **17**, 2148–2156.
42 Y. Z. Wang, Y. Zhao and S. K. Cho, In-droplet magnetic beads concentration and separation for digital microfluidics, 14th International Conference on Solid-State Sensors, Actuators and Microsystems/21st European Conference on Solid-State Transducers, Lyon, FRANCE, 2007.
43 N. Bhalla, W. Y. D. Chung, K. Wang, T. Lessmana and P. Estrela, Electrowetting enabled magnetic particle immunoassay with on-chip magnetic washing, 12th IEEE Sensors Conference, Baltimore, MD, 2013.
44 A. Rival, D. Jary, C. Delattre, Y. Fouillet, G. Castellan, A. Bellemin-Comte and X. Gidrol, *Lab Chip*, 2014, **14**, 3739–3749.
45 J. A. Moore, M. Nemat-Gorgani, A. C. Madison, M. A. Sandahl, S. Punnamaraju, A. E. Eckhardt, M. G. Pollack, F. Vigneault, G. M. Church, R. B. Fair, M. A. Horowitz and P. B. Griffin, *Biomicrofluidics*, 2017, **11**, 014110.
46 A. H. C. Ng, K. Choi, R. P. Luoma, J. M. Robinson and A. R. Wheeler, *Anal. Chem.*, 2012, **84**, 8805–8812.
47 R. S. Sista, A. E. Eckhardt, V. Srinivasan, M. G. Pollack, S. Palanki and V. K. Pamula, *Lab Chip*, 2008, **8**, 2188–2196.
48 M. N. Tsaloglou, A. Jacobs and H. Morgan, *Anal. Bioanal. Chem.*, 2014, **406**, 5967–5976.
49 N. Vergauwe, S. Vermeir, J. B. Wacker, F. Ceyssens, M. Cornaglia, R. Puers, M. A. M. Gijs, J. Lammertyn and D. Wittersaabios, *Sens. Actuators, B*, 2014, **196**, 282–291.
50 K. Jin, C. X. Hu, S. Y. Hu, C. Y. Hu, J. H. Li and H. B. Ma, *Lab Chip*, 2021, **21**, 2892–2900.
51 L. Coudron, M. B. McDonnell, I. Munro, D. K. McCluskey, I. D. Johnston, C. K. L. Tan and M. C. Tracey, *Biosens. Bioelectron.*, 2019, **128**, 52–60.
52 Y. G. Liu and I. Papautsky, *Micromachines*, 2019, **10**, 107.
53 J. Leipert and A. Tholey, *Lab Chip*, 2019, **19**, 3490–3498.
54 A. B. Alias, C. E. Chiang, H. Y. Huang, K. T. Lin, P. J. Lu, Y. W. Wang, T. H. Wu, P. S. Jiang, C. A. Chen and D. J. Yao, *Sci. Rep.*, 2020, **10**, 9708.
55 C. E. Chiang, H. Y. Huang, K. T. Lin, A. B. Alias, P. J. Lu, Y. W. Wang, T. H. Wu, P. S. Jiang, C. A. Chen and D. J. Yao, *Microfluid. Nanofluid.*, 2020, **24**, 55.
56 P. Y. Hung, P. S. Jiang, E. F. Lee, S. K. Fan and Y. W. Lu, *Microsystem Technologies-Micro-and Nanosystems-Information Storage and Processing Systems*, 2017, vol. 23, pp. 313–320.
57 H. H. Shen, T. Y. Su, Y. J. Liu, H. Y. Chang and D. J. Yao, *Sens. Mater.*, 2013, **25**, 643–651.
58 E. R. F. Welch, Y. Y. Lin, A. Madison and R. B. Fair, *Biotechnol. J.*, 2011, **6**, 165–176.
59 Q. Ruan, F. Zou, Y. Wang, Y. Zhang, X. Xu, X. Lin, T. Tian, H. Zhang, L. Zhou, Z. Zhu and C. Yang, *ACS Appl. Mater. Interfaces*, 2021, **13**, 8042–8048.
60 G. J. Shah and C. J. Kim, *Lab Chip*, 2009, **9**, 2402–2405.
61 G. J. Shah, C. J. Kim and Ieee, High-purity separation of rare species in droplet microfluidics using droplet-conduit structures, 22nd International Conference on Micro Electro Mechanical Systems (MEMS), Sorrento, ITALY, 2009.
62 L. Chen and R. B. Fair, *Microfluid. Nanofluid.*, 2015, **19**, 1349–1361.

63 C. Y. Huang, P. Y. Tsai, I. C. Lee, H. Y. Hsu, H. Y. Huang, S. K. Fan, D. J. Yao, C. H. Liu and W. Hsu, *Biomicrofluidics*, 2016, **10**, 011901.
64 J. J. Guo, L. Lin, K. F. Zhao, Y. L. Song, M. J. Huang, Z. Zhu, L. J. Zhou and C. Y. Yang, *Lab Chip*, 2020, **20**, 1577–1585.
65 L. Pang, J. Ding and S.-K. Fan, in *Handbook of Single-Cell Technologies*, ed. T. S. Santra and F.-G. Tseng, Springer Singapore, Singapore, 2022, pp. 185–205, DOI: **10.1007/978-981-10-8953-4_41**.
66 P. Y. Chiou, H. Moon, H. Toshiyoshi, C. J. Kim and M. C. Wu, *Sens. Actuators, A*, 2003, **104**, 222–228.
67 S. Y. Park, M. A. Teitell and E. P. Y. Chiou, *Lab Chip*, 2010, **10**, 1655–1661.
68 D. Y. Jiang, S. Lee, S. W. Bae and S. Y. Park, *Lab Chip*, 2018, **18**, 532–539.
69 D. Y. Jiang and S. Y. Park, *Lab Chip*, 2016, **16**, 1831–1839.
70 C. M. Collier, K. A. Hill, M. A. DeWachter, A. M. Huizing and J. F. Holzman, *J. Biomed. Opt.*, 2015, **20**, 025004.
71 C. Doering, J. Strassner and H. Fouckhardt, *Int. J. Anal. Chem.*, 2022, **2022**, 2011170.
72 S. N. Pei, J. K. Valley, Y. L. Wang and M. C. Wu, *J. Lightwave Technol.*, 2015, **33**, 3486–3493.
73 T. M. Yu, S. M. Yang, C. Y. Fu, M. H. Liu, L. Hsu, H. Y. Chang and C. H. Liu, *Sens. Actuators, B*, 2013, **180**, 35–42.
74 H. S. Chuang, A. Kumar and S. T. Wereley, *Appl. Phys. Lett.*, 2008, **93**, 064104.
75 J. Loo, S. N. Pei and M. C. Wu, *J. Opt. Microsyst.*, 2021, **1**, 034001.
76 S. K. Thio, S. Bae and S. Y. Park, *Sens. Actuators, B*, 2020, **308**, 127704.
77 A. Ashkin, *Phys. Rev. Lett.*, 1970, **24**, 156–159.
78 A. Ashkin, *Science*, 1980, **210**, pp. 1081–1088.
79 D. G. Grier, *Curr. Opin. Colloid Interface Sci.*, 1997, **2**, 264–270.
80 D. Decrop, T. Brans, P. Gijsenbergh, J. D. Lu, D. Spasic, T. Kokalj, F. Beunis, P. Goos, R. Puers and J. Lammertyn, *Anal. Chem.*, 2016, **88**, 8596–8603.
81 P. T. Kumar, D. Decrop, S. Safdar, I. Passaris, T. Kokalj, R. Puers, A. Aertsen, D. Spasic and J. Lammertyn, *Micromachines*, 2020, **11**, 308.
82 P. Y. Chiou, Z. H. Chang and M. C. Wu, A novel opto-electronic tweezer using light induced dielectrophoresis, IEEE/LEOS International Conference on Optical MEMS, Waikoloa, Hi, 2003.
83 G. J. Shah, A. T. Ohta, E. P. Y. Chiou, M. C. Wu and C.-J. Kim, *Lab Chip*, 2009, **9**, 1732–1739.
84 J. K. Valley, N. P. Shao, A. Jamshidi, H. Y. Hsu and M. C. Wu, *Lab Chip*, 2011, **11**, 1292–1297.
85 K. W. Huang, T. W. Su, A. Ozcan and P. Y. Chiou, *Lab Chip*, 2013, **13**, 2278–2284.
86 S. Zhang, M. Elsayed, R. Peng, Y. Chen, Y. Zhang, J. Peng, W. Li, M. D. Chamberlain, A. Nikitina, S. Yu, X. Liu, S. L. Neale and A. R. Wheeler, *Nat. Commun.*, 2021, **12**, 5349.
87 S. H. Au, S. C. C. Shih and A. R. Wheeler, *Biomed. Microdevices*, 2011, **13**, 41–50.
88 K. L. Ho, H. Y. Liao, H. M. Liu, Y. W. Lu, P. K. Yeh, J. Y. Chang and S. K. Fan, *Micromachines*, 2022, **13**, 196.
89 R. Prakash, K. Pabbaraju, S. Wong, R. Tellier and K. Kaler, *Biomed. Microdevices*, 2016, **18**, 44.
90 R. Prakash, K. Pabbaraju, S. Wong, A. Wong, R. Tellier and K. Kaler, *J. Electrochem. Soc.*, 2014, **161**, B3083–B3093.
91 R. Prakash, K. Pabbaraju, S. Wong, A. Wong, R. Tellier and K. Kaler, *Micromachines*, 2015, **6**, 63–79.
92 Y. H. Chang, G. B. Lee, F. C. Huang, Y. Y. Chen and J. L. Lin, *Biomed. Microdevices*, 2006, **8**, 215–225.
93 K. Ugsornrat, N. V. Afzulpurkar, A. Wisitsoraat and A. Tuantranont, *Sens. Mater.*, 2010, **22**, 271–284.
94 K. Ugsornrat, T. Maturus, A. Jomphoak, T. Pogfai, N. V. Afzulpurkar, A. Wisitsoratt and A. Tuantranont, Simulation and Experimental Study of Electrowetting on Dielectric (EWOD) Device for a Droplet Based Polymerase Chain Reaction System, 13th International Conference on Biomedical Engineering (ICBME), SINGAPORE, 2008.
95 B. J. Coelho, B. Veigas, L. Bettencourt, H. Aguas, E. Fortunato, R. Martins, P. V. Baptista and R. Igreja, *Biosensors*, 2022, **12**, 201.
96 T. Hoang, B. H. Ly, T. X. Le, T. T. Huynh, H. T. Nguyen, T. V. Vo, T. T. H. Pham and K. Huynh, *Microsystem Technologies-Micro-and Nanosystems-Information Storage and Processing Systems*, 2020, vol. 26, pp. 1863–1873.
97 S. Y. Hu, Y. H. Jie, K. Jin, Y. F. Zhang, T. J. Guo, Q. Huang, Q. Mei, F. Q. Ma and H. B. Ma, *Biosensors*, 2022, **12**, 324.
98 L. Wan, T. L. Chen, J. Gao, C. Dong, A. H. H. Wong, Y. W. Jia, P. I. Mak, C. X. Deng and R. P. Martins, *Sci. Rep.*, 2017, **7**, 14586.
99 L. Wan, J. Gao, T. L. Chen, C. Dong, H. R. Li, Y. Z. Wen, Z. R. Lun, Y. W. Jia, P. I. Mak and R. P. Martins, *Biomed. Microdevices*, 2019, **21**, 9.
100 J. N. Shen, L. Y. Zhang, J. J. Yuan, Y. S. Zhu, H. Cheng, Y. B. Zeng, J. Q. Wang, X. Q. You, C. Y. Yang, X. M. Qu and H. Chen, *Anal. Chem.*, 2021, **93**, 15033–15041.
101 M. Z. Li, L. Wan, M. K. Law, L. Meng, Y. W. Jia, P. I. Mak and R. P. Martins, *Lab Chip*, 2022, **22**, 537–549.
102 P. C. Gach, S. C. C. Shih, J. Sustarich, J. D. Keasling, N. J. Hillson, P. D. Adams and A. K. Singh, *ACS Synth. Biol.*, 2016, **5**, 426–433.
103 E. Moazami, J. M. Perry, G. Soffer, M. C. Husser and S. C. C. Shih, *Anal. Chem.*, 2019, **91**, 5159–5168.
104 J. M. Perry, G. Soffer, R. Jain and S. C. C. Shih, *Lab Chip*, 2021, **21**, 3730–3741.
105 G. Sathyanarayanan, M. Haapala, I. Kiiski and T. Sikanen, *Anal. Bioanal. Chem.*, 2018, **410**, 6677–6687.
106 S. C. C. Shih, G. Goyal, P. W. Kim, N. Koutsoubelis, J. D. Keasling, P. D. Adams, N. J. Hillson and A. K. Singh, *ACS Synth. Biol.*, 2015, **4**, 1151–1164.
107 Z. P. Li, T. Y. Ho and K. Chakrabarty, Optimization of Heaters in a Digital Microfluidic Biochip for the Polymerase Chain Reaction, 20th International Workshop

on Thermal Investigations of ICs and Systems (THERMINIC), Greenwich, ENGLAND, 2014.
108 H. Norian, R. M. Field, I. Kymissis and K. L. Shepard, *Lab Chip*, 2014, **14**, 4076–4084.
109 H. H. Shen, T. Y. Su, H. Y. Chang and D. J. Yao, SNP Detection based on Temperature-Controllable EWOD Digital Microfluidics System, IEEE Nanotechnology Materials and Devices Conference (IEEE NMDC), Honolulu, HI, 2012.
110 S. Chen, P. Y. Keng, R. M. van Dam and C. J. Kim, Synthesis of f-18-labeled probes on ewod platform for positron emission tomography (pet) preclinical imaging, 24th IEEE International Conference on Micro Electro Mechanical Systems (MEMS), Cancun, MEXICO, 2011.
111 S. P. Chen, M. R. Javed, H. K. Kim, J. Lei, M. Lazari, G. J. Shah, R. M. van Dam, P. Y. Keng and C. J. Kim, *Lab Chip*, 2014, **14**, 902–910.
112 K. N. Nampoothiri, M. S. Seshasayee, V. Srinivasan, M. S. Bobji and P. Sen, *Sens. Actuators, B*, 2018, **273**, 862–872.
113 W. Nelson, I. Peng, J. A. Loo, R. L. Garrell and C. J. Kim, An ewod droplet microfluidic chip with integrated local temperature control for multiplex proteomics, 22nd International Conference on Micro Electro Mechanical Systems (MEMS), Sorrento, ITALY, 2009.
114 W. C. Nelson, I. Peng, G. A. Lee, J. A. Loo, R. L. Garrell and C. J. Kim, *Anal. Chem.*, 2010, **82**, 9932–9937.
115 M. J. Jebrail, R. F. Renzi, A. Sinha, J. Van De Vreugde, C. Gondhalekar, C. Ambriz, R. J. Meagher and S. S. Branda, *Lab Chip*, 2015, **15**, 151–158.
116 B. Grigoryan, S. J. Paulsen, D. C. Corbett, D. W. Sazer, C. L. Fortin, A. J. Zaita, P. T. Greenfield, N. J. Calafat, J. P. Gounley, A. H. Ta, F. Johansson, A. Randles, J. E. Rosenkrantz, J. D. Louis-Rosenberg, P. A. Galie, K. R. Stevens and J. S. Miller, *Science*, 2019, **364**, 458–464.
117 J. McGrath, M. Jimenez and H. Bridle, *Lab Chip*, 2014, **14**, 4139–4158.
118 Y.-T. Kang, E. Purcell, C. Palacios-Rolston, T.-W. Lo, N. Ramnath, S. Jolly and S. Nagrath, *Small*, 2019, **15**, 1903600.
119 Y. X. Lu, L. Ye, X. Y. Jian, D. W. Yang, H. W. Zhang, Z. D. Tong, Z. H. Wu, N. Shi, Y. W. Han and H. J. Mao, *Biosens. Bioelectron.*, 2022, **204**, 113879.
120 I. Barbulovic-Nad, S. H. Au and A. R. Wheeler, *Lab Chip*, 2010, **10**, 1536–1542.
121 A. H. C. Ng, M. D. Chamberlain, H. Situ, V. Lee and A. R. Wheeler, *Nat. Commun.*, 2015, **6**, 7513.
122 X. Xu, Q. Zhang, J. Song, Q. Ruan, W. Ruan, Y. Chen, J. Yang, X. Zhang, Y. Song, Z. Zhu and C. Yang, *Anal. Chem.*, 2020, **92**, 8599–8606.
123 D. Witters, K. Knez, F. Ceyssens, R. Puers and J. Lammertyn, *Lab Chip*, 2013, **13**, 2047–2054.
124 S. H. Au, M. D. Chamberlain, S. Mahesh, M. V. Sefton and A. R. Wheeler, *Lab Chip*, 2014, **14**, 3290–3299.
125 J. Zhai, H. Li, A. H.-H. Wong, C. Dong, S. Yi, Y. Jia, P.-I. Mak, C.-X. Deng and R. P. Martins, *Microsyst. Nanoeng.*, 2020, **6**, 6.
126 J. Zhai, H. Li, A. H.-H. Wong, C. Dong, S. Yi, Y. Jia, P.-I. Mak, C. Deng and R. P. Martins, *Bio-Protoc.*, 2020, **10**, e3769–e3769.
127 Q. Ruan, W. Ruan, X. Lin, Y. Wang, F. Zou, L. Zhou, Z. Zhu and C. Yang, *Sci. Adv.*, 2020, **6**, eabd6454.
128 J. Zhai, C. Li, H. Li, S. Yi, N. Yang, K. Miao, C. Deng, Y. Jia, P.-I. Mak and R. P. Martins, *Lab Chip*, 2021, **21**, 4749–4759.
129 B. F. Bender, A. P. Aijian and R. L. Garrell, *Lab Chip*, 2016, **16**, 1505–1513.
130 A. Das, C. Weise, M. Polack, R. D. Urban, B. Krafft, S. Hasan, H. Westphal, R. Warias, S. Schmidt, T. Gulder and D. Belder, *J. Am. Chem. Soc.*, 2022, **144**, 10353–10360.
131 A. E. Kirby and A. R. Wheeler, *Lab Chip*, 2013, **13**, 2533–2540.
132 R. Pethig, *Biomicrofluidics*, 2010, **4**, 022811.
133 B. Cetin and D. Q. Li, *Electrophoresis*, 2011, **32**, 2410–2427.
134 K. Khoshmanesh, S. Nahavandi, S. Baratchi, A. Mitchell and K. Kalantar-zadeh, *Biosens. Bioelectron.*, 2011, **26**, 1800–1814.
135 D. Chatterjee, H. Shepherd and R. L. Garrell, *Lab Chip*, 2009, **9**, 1219–1229.
136 K. Kaler, R. Prakash and D. Chugh, *Biomicrofluidics*, 2010, **4**, 022805.
137 S. K. Fan, T. H. Hsieh and D. Y. Lin, *Lab Chip*, 2009, **9**, 1236–1242.
138 S.-K. Fan, P.-W. Huang, T.-T. Wang and Y.-H. Peng, *Lab Chip*, 2008, **8**, 1325–1331.
139 H. Nejad and M. Hoorfar, *Microfluid. Nanofluid.*, 2015, **18**, 483–492.
140 H. R. Nejad, O. Z. Chowdhury, M. D. Buat and M. Hoorfar, *Lab Chip*, 2013, **13**, 1823–1830.
141 B. A. Nestor, E. Samiei, R. Samanipour, A. Gupta, A. Van den Berg, M. D. de Leon Derby, Z. Wang, H. R. Nejad, K. Kim and M. Hoorfar, *RSC Adv.*, 2016, **6**, S7409–S7416.
142 T. Komatsu, M. Tokeshi and S. K. Fan, *Biosens. Bioelectron.*, 2022, **195**, 113631.
143 J. A. Balasingam, S. Swaminathan, H. Nazemi, C. Love, Y. Birjis and A. Emadi, in *Encyclopedia of Sensors and Biosensors*, ed. R. Narayan, Elsevier, Oxford, 1st edn, 2023, pp. 209–225, DOI: **10.1016/B978-0-12-822548-6.00001-7**.
144 M. V. Voinova, *J. Sens.*, 2009, **2009**, 943125.
145 S. P. Zhang, J. Lata, C. Y. Chen, J. Mai, F. Guo, Z. H. Tian, L. Q. Ren, Z. M. Mao, P. H. Huang, P. Li, S. J. Yang and T. J. Huang, *Nat. Commun.*, 2018, **9**, 2928.
146 H. D. Zhu, P. R. Zhang, Z. W. Zhong, J. P. Xia, J. Rich, J. Mai, X. Y. Su, Z. H. Tian, H. Bachman, J. Rufo, Y. Y. Gu, P. T. Kang, K. Chakrabarty, T. P. Witelski and T. J. Huang, *Sci. Adv.*, 2021, **7**, eabc7885.
147 M. L. Zhang, J. Z. Huang, Y. Lu, W. Pang, H. Zhang and X. X. Duan, *ACS Sens.*, 2018, **3**, 1584–1591.
148 M. L. Zhang, W. W. Cui, X. J. Chen, C. Wang, W. Pang, X. X. Duan, D. H. Zhang and H. Zhang, *J. Micromech. Microeng.*, 2015, **25**, 025002.
149 Y. Lu, M. L. Zhang, H. X. Zhang, J. Z. Huang, Z. Wang, Z. L. Yun, Y. Y. Wang, W. Pang, X. X. Duan and H. Zhang, *Microfluid. Nanofluid.*, 2018, **22**, 146.

150 A. C. Madison, M. W. Royal and R. B. Fair, *Microfluid. Nanofluid.*, 2017, **21**, 176.
151 Y. Li, Y. Q. Fu, S. D. Brodie, M. Alghane and A. J. Walton, *Biomicrofluidics*, 2012, **6**, 012812.
152 Y. F. Li, R. Y. Fu, D. Winters, B. W. Flynn, B. Parkes, D. S. Brodie, Y. F. Liu, J. Terry, L. I. Haworth, A. S. Bunting, J. T. M. Stevenson, S. Smith, C. L. Mackay, P. R. R. Langridge-Smith, A. A. Stokes and A. J. Walton, *IEEE Trans. Semicond. Manuf.*, 2012, **25**, 323–330.
153 T. Won, D. Jang, K. Y. Lee and S. K. Chung, *J. Microelectromech. Syst.*, 2021, **30**, 783–790.
154 S. K. Chung and S. K. Cho, *J. Micromech. Microeng.*, 2008, **18**, 125024.
155 S. Bansal and S. Subramanian, *Adv. Mater. Technol.*, 2021, **6**, 2100491.
156 M. A. Murran and H. Najjaran, *Lab Chip*, 2012, **12**, 2053–2059.
157 S. C. C. Shih, R. Fobel, P. Kumar and A. R. Wheeler, *Lab Chip*, 2011, **11**, 535–540.
158 Q. F. Zhu, Y. X. Lu, S. T. Xie, Z. J. Luo, S. T. Shen, Z. B. Yan, M. L. Jin, G. F. Zhou and L. L. Shui, *Microfluid. Nanofluid.*, 2020, **24**, 59.
159 J. Gong, S. K. Fan and C. J. Kim, Portable digital microfluidics platform with active but disposable lab-on-chip, Maastricht, 17th IEEE International Conference on Micro Electro Mechanical Systems, Maastricht, NETHERLANDS, 2004.
160 B. Bhattacharjee and H. Najjaran, *Lab Chip*, 2012, **12**, 4416–4423.
161 S. C. C. Shih, I. Barbulovic-Nad, X. N. Yang, R. Fobel and A. R. Wheeler, *Biosens. Bioelectron.*, 2013, **42**, 314–320.
162 E. Scott-Murrell, D. Lanza and M. J. Schertzer, *Microsystem Technologies-Micro-and Nanosystems-Information Storage and Processing Systems*, 2017, vol. 23, pp. 3131–3139.
163 J. Gao, X. M. Liu, T. L. Chen, P. I. Mak, Y. G. Du, M. I. Vai, B. C. Lin and R. P. Martins, *Lab Chip*, 2013, **13**, 443–451.
164 S. Han, X. M. Liu, L. Wang, Y. H. Wang and G. X. Zheng, *MethodsX*, 2019, **6**, 1443–1453.
165 S. Han, Q. Zhang, X. C. Zhang, X. M. Liu, L. Lu, J. F. Wei, Y. C. Li, Y. H. Wang and G. X. Zheng, *Biosens. Bioelectron.*, 2019, **143**, 111597.
166 Q. Zhang, X. C. Zhang, X. L. Zhang, L. Jiang, J. M. Yin, P. Zhang, S. Han, Y. H. Wang and G. X. Zheng, *Mar. Pollut. Bull.*, 2019, **144**, 20–27.
167 Z. J. Luo, J. J. Fan, B. R. Huang, S. Y. Liu and F. Dai, *Asia–Pac. J. Chem. Eng.*, 2020, **15**, e2449.
168 Z. J. Luo, B. R. Huang, J. Z. Xu, L. Wang, Z. T. Huang, L. Cao and S. Y. Liu, *Open Chem.*, 2021, **19**, 665–677.
169 X. B. Wang, Y. H. Piao, Y. Su and W. Q. Wang, *Microfluid. Nanofluid.*, 2018, **22**, 129.
170 I. Spotts, D. Ismail, N. Jaffar and C. M. Collier, *Sens. Actuators, A*, 2018, **280**, 164–169.
171 K. Choi, J. Y. Kim, J. H. Ahn, J. M. Choi, M. Im and Y. K. Choi, *Lab Chip*, 2012, **12**, 1533–1539.
172 K. M. Lei, P. I. Mak, M. K. Law and R. P. Martins, *Analyst*, 2014, **139**, 6204–6213.
173 K. M. Lei, P. I. Mak, M. K. Law and R. P. Martins, *Analyst*, 2015, **140**, 5129–5137.
174 K. M. Lei, P. I. Mak, M. K. Law and R. P. Martins, *IEEE J. Solid-State Circuits*, 2016, **51**, 2274–2286.
175 Y. Mashraei, S. Sivashankar, U. Buttner and K. N. Salama, *IEEE Sens. J.*, 2016, **16**, 8775–8783.
176 Y. Yu, R. P. S. de Campos, S. Hong, D. L. Krastev, S. Sadanand, Y. Leung and A. R. Wheeler, *Microsyst. Nanoeng.*, 2019, **5**, 10.
177 Y. Yu, M. H. Shamsi, D. L. Krastev, M. D. M. Dryden, Y. Leung and A. R. Wheeler, *Lab Chip*, 2016, **16**, 543–552.
178 C. Karuwan, K. Sukthang, A. Wisitsoraat, D. Phokharatkul, V. Patthanasettakul, W. Wechsatol and A. Tuantranont, *Talanta*, 2011, **84**, 1384–1389.
179 M. H. Shamsi, K. Choi, A. H. C. Ng and A. R. Wheeler, *Lab Chip*, 2014, **14**, 547–554.
180 D. G. Rackus, M. D. M. Dryden, J. Lamanna, A. Zaragoza, B. Lam, S. O. Kelley and A. R. Wheeler, *Lab Chip*, 2015, **15**, 3776–3784.
181 Y. H. Yu, J. F. Chen and J. Zhou, *J. Micromech. Microeng.*, 2014, **24**, 015020.
182 A. Farzbod and H. Moon, *Biosens. Bioelectron.*, 2018, **106**, 37–42.
183 R. P. S. de Campos, D. G. Rackus, R. Shih, C. Zhao, X. Liu and A. R. Wheeler, *Anal. Chem.*, 2019, **91**, 2506–2515.
184 M. Abdelgawad, M. W. L. Watson and A. R. Wheeler, *Lab Chip*, 2009, **9**, 1046–1051.
185 M. W. L. Watson, M. J. Jebrail and A. R. Wheeler, *Anal. Chem.*, 2010, **82**, 6680–6686.
186 A. Abadian, S. S. Manesh and S. J. Ashtiani, *Microfluid. Nanofluid.*, 2017, **21**, 65.
187 C. Wu, F. Brunelle, M. Harnois, J. Follet and V. Senez, An integrated hybrid microfluidic system for online bioprocesses monitoring: combining electrical lysis and ewod sample preparation, 25th IEEE International Conference on Micro Electro Mechanical Systems (MEMS), Paris, FRANCE, 2012.
188 S. C. C. Shih, P. C. Gach, J. Sustarich, B. A. Simmons, P. D. Adams, S. Singh and A. K. Singh, *Lab Chip*, 2015, **15**, 225–236.
189 H. Gu, M. H. G. Duits and F. Mugele, *Lab Chip*, 2010, **10**, 1550–1556.
190 K. Samlali, F. Ahmadi, A. B. V. Quach, G. Soffer and S. C. C. Shih, *Small*, 2020, **16**, 2002400.
191 R. Renaudot, V. Agache, Y. Fouillet, G. Laffite, E. Bisceglia, L. Jalabert, M. Kumemura, D. Collard and H. Fujita, *Lab Chip*, 2013, **13**, 4517–4524.
192 M. J. Ahamed, R. Ben-Mrad and P. Sullivan, *J. Microelectromech. Syst.*, 2013, **22**, 536–541.
193 S. K. Vashist and J. H. T. Luong, in *Handbook of Immunoassay Technologies*, ed. S. K. Vashist and J. H. T. Luong, Academic Press, 2018, pp. 1–18, DOI: **10.1016/B978-0-12-811762-0.00001-3**.

194 A. H. C. Ng, R. Fobel, C. Fobel, J. Lamanna, D. G. Rackus, A. Summers, C. Dixon, M. D. M. Dryden, C. Lam, M. Ho, N. S. Mufti, V. Lee, M. A. M. Asri, E. A. Sykes, M. D. Chamberlain, R. Joseph, M. Ope, H. M. Scobie, A. Knipes, P. A. Rota, N. Marano, P. M. Chege, M. Njuguna, R. Nzunza, N. Kisangau, J. Kiogora, M. Karuingi, J. W. Burton, P. Borus, E. Lam and A. R. Wheeler, *Sci. Transl. Med.*, 2018, **10**, eaar6076.

195 A. A. Sklavounos, J. Lamanna, D. Modi, S. Gupta, A. Mariakakis, J. Callum and A. R. Wheeler, *Clin. Chem.*, 2021, **67**, 1699–1708.

196 N. Ali, R. D. P. Rampazzo, A. D. T. Costa and M. A. Krieger, *BioMed Res. Int.*, 2017, 9306564.

197 S. Y. Chen, Y. C. Sun, F. F. Fan, S. L. Chen, Y. R. Zhang, Y. Zhang, X. L. Meng and J. M. Lin, *TrAC, Trends Anal. Chem.*, 2022, **157**, 116737.

198 Y. X. Zhao, F. Chen, Q. Li, L. H. Wang and C. H. Fan, *Chem. Rev.*, 2015, **115**, 12491–12545.

199 A. Ahmadian, M. Ehn and S. Hober, *Clin. Chim. Acta*, 2006, **363**, 83–94.

200 J. Shendure and H. L. Ji, *Nat. Biotechnol.*, 2008, **26**, 1135–1145.

201 A. Carrel, *J. Exp. Med.*, 1912, **16**, 165–168.

202 J.-L. He, A.-T. Chen, J.-H. Lee and S.-K. Fan, *Int. J. Mol. Sci.*, 2015, **16**, 22319–22332.

203 A. E. Kirby and A. R. Wheeler, *Anal. Chem.*, 2013, **85**, 6178–6184.

204 A. R. Wheeler, H. Moon, C. A. Bird, R. R. O. Loo, C. J. Kim, J. A. Loo and R. L. Garrell, *Anal. Chem.*, 2005, **77**, 534–540.

205 A. R. Wheeler, H. Moon, C. J. Kim, J. A. Loo and R. L. Garrell, *Anal. Chem.*, 2004, **76**, 4833–4838.

206 F. Lapierre, G. Piret, H. Drobecq, O. Melnyk, Y. Coffinier, V. Thomy and R. Boukherroub, *Lab Chip*, 2011, **11**, 1620–1628.

207 G. Perry, F. Lapierre, Y. Coffinier, V. Thomy, R. Boukherroub, C. X. Lu, S. H. Tsang, B. K. Tay, P. Coquet and Ieee, Droplet based lab-on-chip microfluidic microsystems integrated nanostructured surfaces for high sensitive mass spectrometry analysis, 5th IEEE International Nanoelectronics Conference (IEEE INEC), Singapore, SINGAPORE, 2013.

208 I. Jang, H. Ko, G. You, H. Lee, S. Paek, H. Chae, J. H. Lee, S. Choi, O. S. Kwon, K. Shin and H. B. Oh, *BioChip J.*, 2017, **11**, 146–152.

209 O. Kudina, H. B. Eral and F. Mugele, *J. Mass Spectrom.*, 2017, **52**, 405–410.

210 O. Kudina, B. Eral and F. Mugele, *Anal. Chem.*, 2016, **88**, 4669–4675.

211 Q. Y. Ruan, J. Yang, F. X. Zou, X. F. Chen, Q. Q. Zhang, K. F. Zhao, X. Y. Lin, X. Zeng, X. Y. Yu, L. L. Wu, S. C. Lin, Z. Zhu and C. Y. Yang, *Anal. Chem.*, 2022, **94**, 1108–1117.

212 C. A. Baker and M. G. Roper, *Anal. Chem.*, 2012, **84**, 2955–2960.

213 J. B. Hu, T. R. Chen, C. H. Chang, J. Y. Cheng, Y. C. Chen and P. L. Urban, *Analyst*, 2015, **140**, 1495–1501.